J. Am. Chem. Soc. **1991**, *113*, 74-87

Activation to the Transition State: Reactant and Solvent Energy Flow for a Model S_N2 Reaction in Water

Bradley J. Gertner,[†] Robert M. Whitnell,[†] Kent R. Wilson,[*,†] and James T. Hynes[*,‡]

Contribution from the Department of Chemistry, University of California, San Diego, La Jolla, California 92093-0339, and Department of Chemistry and Biochemistry, University of Colorado, Boulder, Colorado 80309-0215. *Received April 20, 1990*

Abstract: We have performed molecular dynamics calculations on a model $Cl^- + CH_3Cl$ S_N2 reaction in water in order to elucidate how the reactants obtain sufficient energy from the solvent to climb the potential energy barrier to reaction. This system, consisting of ionic and dipolar reagents in a polar solvent, is representative of a large class of chemical reactions with strong Coulombic reagent–solvent coupling. We find that the change in internal energy of the reactants during the barrier-climbing process involves three distinct epochs: (i) vibrational activation of the methyl chloride in the initial Cl^-CH_3Cl ion–dipole complex, (ii) gradual increase in kinetic and potential energies of the reactants, and (iii) fast dumping of reactant kinetic energy into reactant potential energy resulting in the reactants reaching the top of the potential energy barrier, with the symmetric structure $Cl^{\delta-}CH_3^{\delta+}Cl^{\delta-}$. The energy that the reagents gain during this process comes primarily from the potential energy of the water solvent. We also show that many water molecules are involved in this energy transfer, but almost as much energy is removed from the reactants by these water molecules as is deposited in them over the course of the barrier climbing. The critical change in the charge distribution as the reactants climb the barrier occurs over a very short time, and we present evidence that the total energy of the water solvent molecules remains essentially constant, consistent with the frozen solvent nonadiabatic solvation model used previously to understand the deviations from the transition-state rate for this system (Bergsma et al. *J. Chem. Phys.* **1987**, *86*, 1356; Gertner et al. *J. Chem. Phys.* **1987**, *86*, 1377; **1989**, *90*, 3537). We also find that the water solvent undergoes a substantial, though not complete, reorganization well before the change in the charge distribution of the reactants. This reorganization is crucial, although not sufficient, for the success of the barrier climbing. Many of these results for this strongly coupled system contrast starkly with those found by Benjamin et al. (*J. Am. Chem. Soc.* **1990**, *112*, 524) for a neutral symmetric atom exchange reaction in a rare gas solvent (Bergsma et al. *Chem. Phys. Lett.* **1986**, *123*, 394; *J. Chem. Phys.* **1986**, *85*, 5625) where the forces between solvent and reagents are short range and the coupling is much weaker. Thus, there is a rich variety of energy flow phenomena and solvent dynamics that must be considered in order to understand the detailed molecular dynamics of how chemical reactions take place in solution and how these dynamics arise from the particular system's reagent, solvent, and solvent–reagent forces.

I. Introduction

For an activated chemical reaction to occur in solution, there must be an energy flow from the solvent to the reactants. In this paper, we examine the mechanisms and time scales of this process for a model S_N2 nucleophilic displacement reaction in water. In particular, for the reaction

$$Cl^- + CH_3Cl \rightarrow ClCH_3 + Cl^- \tag{1}$$

we study how the chloride ion plus methyl chloride molecule reactants climb the potential energy barrier to reach the transition state and how the surrounding water molecules aid, abet, and sometimes hinder this ascent.

In many discussions, such reactions are portrayed as passage over a barrier in free energy along some reaction coordinate. By contrast, here we wish to move beyond this usual concept of "reaction mechanism" by following the reaction at a molecular level through the computation, via molecular dynamics (MD), of the microscopic atomic trajectories for the reacting species and the solvent molecules. The questions we pose and answer include the following: How long does it take for the system to climb the barrier? Are there different time scales and time sequences for the reagents in contrast to the participation of the solvent, or does the activation of the reaction proceed in a more concerted fashion? Which modes of solvent energy are used to drive the reactants up the barrier, and which modes of the reactants receive this energy and are involved in climbing the barrier? The answers to such questions are essential in providing a molecular level picture of the reaction dynamics in solution, but they are difficult to access directly with current experimental techniques. Indeed, it is only due to the advances in computational power over the last few years that these issues can even be examined in a computer simulation.

The computational study of the aqueous $Cl^- + CH_3Cl$ reaction at the detailed molecular level began with the calculation using a Monte Carlo simulation technique of the equilibrium potential of mean force along a selected reaction coordinate by Jorgensen and co-workers.[1,2] This is the free energy of the system constructed by imposing the condition that the water solvent molecules are equilibrated to the Cl^-–CH_3Cl system at a given value of the reaction coordinate. Rossky and co-workers[3,4] have also calculated the potential of mean force for this system by using an efficient integral equation technique, while Karplus and co-workers[5] have addressed this calculation with a free energy perturbation technique taking into account quantum mechanical contributions of a core region using semiempirical methods. Warshel and co-workers[6] have used a combination of molecular dynamics and free energy perturbation to study the activation free energy of this system. In addition, Karplus and co-workers[5] and Warshel and co-workers[6,7] have studied the effect of reagent polarization on these free energies and on the water solvent and S_N2 reagent dynamics.

The free energy, or potential of mean force, curve provides, by its values at the transition state and in the reagents' potential energy well, a key piece of information—the reaction activation free energy. Within the framework of transition-state theory (TST), knowledge of this curve at the transition state and in the well of the reactants is sufficient to determine the rate constant

---

[†] University of California, San Diego.

[‡] University of Colorado.

(1) Chandrasekhar, J.; Smith, S. F.; Jorgensen, W. L. *J. Am. Chem. Soc.* **1984**, *106*, 3049.

(2) Chandrasekhar, J.; Smith, S. F.; Jorgensen, W. L. *J. Am. Chem. Soc.* **1985**, *107*, 154.

(3) Chiles, R. A.; Rossky, P. J. *J. Am. Chem. Soc.* **1984**, *106*, 6867.

(4) Huston, S. E.; Rossky, P. J.; Zichi, D. A. *J. Am. Chem. Soc.* **1989**, *111*, 5680.

(5) Bash, P. A.; Field, M. J.; Karplus, M. *J. Am. Chem. Soc.* **1987**, *109*, 8092.

(6) Hwang, J.-K.; King, G.; Creighton, S.; Warshel, A. *J. Am. Chem. Soc.* **1988**, *110*, 5297.

(7) Hwang, J.-K.; Creighton, S.; King, G.; Whitney, D.; Warshel, A. *J. Chem. Phys.* **1988**, *89*, 859.

k^{TST} for the reaction and thereby the magnitude of the overall time required for the reactants to climb the barrier from an equilibrium state.[8]

Examination of the role of the solvent dynamics for this reaction in causing departures from the TST rate, and in accounting for the non-TST feature that the reaction dynamics near the transition state do not in fact occur on this equilibrium free energy curve, was initiated in a series of papers by Wilson, Hynes, and co-workers.[9-12] Those efforts examined the S_N2 system through calculation of the detailed molecular dynamics of the solvent plus reagent system and examined the solvent induced recrossing of the barrier top and its description by analytic rate theories.[10,13-17] In the present work, the focus is shifted to the questions of how the system reaches the transition state via energy flow from the solvent to the reagents and in what time frame and sequence this energy flow occurs. Since energy flow is de facto a question of dynamics, and since the reagents and solvent molecules involved in reactive trajectories are equilibrated neither separately nor with each other, the free energy (potential of mean force) curve is inappropriate for framing, let alone answering, these questions concerning the detailed behavior of the energy flow which, as we shall show, has important components which occur on a much shorter time scale than the overall macroscopic reaction time, approximately k^{-1}.

These issues of energy flow and transition-state attainment have been previously examined at the detailed level of molecular dynamics for a model neutral atom transfer $A + BC \rightarrow AB + C$ reaction in nonpolar rare gas solvents.[18-21] (Some of the results on energy flow from solvent to reagents from ref 20 and the present work have been previewed by Wilson and Levine[30] in a more general discussion of how solvent fluctuations drive activated chemical reactions.) But compared to the earlier study[20] of energy flow for a model $Cl + Cl_2$ reaction in rare gas solution, and as we will stress throughout this work, the aqueous $Cl^- + CH_3Cl$ S_N2 reaction differs qualitatively in almost all respects in its route to the transition state. The source of these differences is simple: there are strong electrostatic forces among the reagent charge transfer $Cl^- + CH_3Cl$ system and the polar water molecules that comprise the solvent.[31] This strong coupling between the reagents and the solvent (and within the solvent itself) leads, as we will show, to several essential features of the barrier-climbing dynamics absent in a "weak coupling" neutral atom transfer in a nonpolar solvent where short range forces are the main form of solvent–reagent and solvent–solvent interaction. The most obvious feature that we will establish in the S_N2 reaction is that many water solvent molecules participate in transferring energy to the reagents. In addition, we find that it is the potential energy of the solvent (rather than the solvent kinetic energy as in the weak coupling case[20]) that provides the majority of the increase in total energy of the reagents necessary for the reagents to climb the barrier. Finally, we will show that the solvent dynamics in the strong coupling system include a reorganization to configurations close to those appropriate for solvating the symmetric charge distribution of the reagents at the transition state ($Cl^{\delta-}CH_3{}^{\delta+}Cl^{\delta-}$) well before the reactants have climbed the barrier. This extensive prior reorganization of the water solvent, which is necessary for the success of the barrier climbing in this system, is much less important in the weak coupling system.

It is useful to specify now in greater detail the process[9,12] we will study. We consider an ensemble of systems which at a time defined to be $t = 0$ all have a value of the reaction coordinate which lies on the transition state surface. For this S_N2 reaction, this means that at $t = 0$, the reagents have a value of the asymmetric stretch equal to zero and therefore have a symmetric charge distribution which we shall denote as $[Cl^{\delta-}CH_3{}^{\delta+}Cl^{\delta-}]$. The positions and velocities of the other degrees of freedom of the reagents as well as the water solvent molecules belong to a Maxwell–Boltzmann distribution at 298 K. Thus, at $t = 0$ the solvent is equilibrated to the S_N2 reagents with a symmetric charge distribution $[Cl^{\delta-}CH_3{}^{\delta+}Cl^{\delta-}]$ at the top of the barrier.

At some time earlier than $t = 0$, each member of the ensemble will be on either the reactant or product side of the reaction barrier. (For this S_N2 reaction, the fate of each trajectory is in fact decided within 50 fs, although it takes somewhat longer for the system to reach the bottom of the potential energy barrier.[9,12]) At this earlier time, the reagents are in the solvated ion–dipole complex $[Cl^-CH_3Cl]$. In this work, we follow the dynamics of this reaction to a time (−500 fs) at which energy is not being appreciably transferred into or removed from the S_N2 reagents by the water solvent. The dynamics for $t > 0$ can be treated similarly.

The S_N2 reaction we study can therefore be depicted as follows. We have an ensemble of systems which at $t = -500$ fs have the reagents in the solvated ion–dipole complex Cl^-CH_3Cl. Because the reaction is symmetric, we can always consider this to be the reactant side of the barrier. The key is that at $t = 0$, *each* member of this ensemble will be at the transition state with the reagents in the symmetric charge distribution $Cl^{\delta-}CH_3{}^{\delta+}Cl^{\delta-}$ and the solvent equilibrated to this distribution. At $t = 500$ fs, each member of the ensemble will be on either the reactant or product side of the barrier. By examining the classical trajectory of each system from $t = -500$ to $t = 500$ fs, we can determine whether a reactive event has taken place and thereby obtain and analyze an ensemble of reactive events. Further, we can regard $t = -500$ fs as the starting point for trajectories that attain the barrier top at $t = 0$.

The outline of this paper is as follows. In sections II and III, we describe respectively the potential energy models for the S_N2

---

(8) Hynes, J. T. In *The Theory of Chemical Reaction Dynamics*; Baer, M., Ed.; CRC Press: Boca Raton, FL, 1985; Vol. IV, p 171.

(9) Bergsma, J. P.; Gertner, B. J.; Wilson, K. R.; Hynes, J. T. *J. Chem. Phys.* **1987**, *86*, 1356.

(10) Gertner, B. J.; Bergsma, J. P.; Wilson, K. R.; Lee, S.; Hynes, J. T. *J. Chem. Phys.* **1987**, *86*, 1377.

(11) Gertner, B. J.; Wilson, K. R.; Zichi, D. A.; Lee, S.; Hynes, J. T. *Discuss. Faraday Soc.* **1988**, *85*, 297.

(12) Gertner, B. J.; Wilson, K. R.; Hynes, J. T. *J. Chem. Phys.* **1989**, *90*, 3537.

(13) Kramers, H. A. *Physica* **1940**, *7*, 284.

(14) Grote, R. F.; Hynes, J. T. *J. Chem. Phys.* **1980**, *73*, 2715.

(15) van der Zwan, G.; Hynes, J. T. *J. Chem. Phys.* **1982**, *76*, 2993.

(16) van der Zwan, G.; Hynes, J. T. *J. Chem. Phys.* **1983**, *78*, 4174.

(17) van der Zwan, G.; Hynes, J. T. *Chem. Phys.* **1984**, *90*, 21.

(18) Bergsma, J. P.; Edelsten, P. M.; Gertner, B. J.; Huber, K. R.; Reimers, J. R.; Wilson, K. R.; Wu, S. M.; Hynes, J. T. *Chem. Phys. Lett.* **1986**, *123*, 394.

(19) Bergsma, J. P.; Reimers, J. R.; Wilson, K. R.; Hynes, J. T. *J. Chem. Phys.* **1986**, *85*, 5625.

(20) Benjamin, I.; Gertner, B. J.; Tang, N. J.; Wilson, K. R. *J. Am. Chem. Soc.* **1990**, *112*, 524.

(21) The studies of the relaxation path of molecular iodine in solution can be viewed in this light as well.[22-29]

(22) Nesbitt, D. J.; Hynes, J. T. *Chem. Phys. Lett.* **1981**, *82*, 252.

(23) Nesbitt, D. J.; Hynes, J. T. *J. Chem. Phys.* **1982**, *76*, 6002.

(24) Nesbitt, D. J.; Hynes, J. T. *J. Chem. Phys.* **1982**, *77*, 2130.

(25) Bado, P.; Berens, P. H.; Bergsma, J. P.; Wilson, S. B.; Wilson, K. R.; Heller, E. J. In *Picosecond Phenomena III*; Eisenthal, K. B., Hochstrasser, R. M., Kaiser, W., Laubereau, A., Eds.; Springer-Verlag: Berlin, 1982; p 260.

(26) Bado, P.; Berens, P. H.; Wilson, K. R. *Proc. Soc. Photo-Optic. Instrum. Eng.* **1982**, *322*, 230.

(27) Bado, P.; Berens, P. H.; Bergsma, J. P.; Coladonato, M. H.; Dupuy, C. G.; Edelsten, P. M.; Kahn, J. D.; Wilson, K. R.; Fredkin, D. R. *Laser Chem.* **1983**, *3*, 231.

(28) Brown, J. K.; Harris, C. B.; Tully, J. C. *J. Chem. Phys.* **1988**, *89*, 6687.

(29) Harris, A. L.; Brown, J. K.; Harris, C. B. *Annu. Rev. Phys. Chem.* **1988**, *39*, 341.

(30) Wilson, K. R.; Levine, R. D. *Chem. Phys. Lett.* **1988**, *152*, 435.

(31) A note concerning terminology: We use the term "strong coupling" to denote solvent–reagent and solvent–solvent interactions that usually involve strong forces that are long range compared to the distance between atoms. The characteristic feature of strong coupling systems is that even small motion of an atom is likely to have some significant, immediate effect on many other atoms. "Weak coupling", on the other hand, denotes interactions that are in general weak and short range. Large forces can occur in weak coupling systems but usually as the result of a rare event—for example, a product atom coming off a high potential energy barrier and undergoing a high energy impulsive collision with a solvent atom. However, small, low velocity motions are unlikely to affect significantly the rest of the system. One can think of the strong coupling system in extremis as masses interconnected with springs; a weak coupling system, on the other hand, is analogous to a set of billiard balls. By these definitions, the S_N2 system in water studied here is a strong coupling system; the $Cl + Cl_2$ system in Ar studied previously[18-20] is weak coupling.

reaction system and details of the molecular dynamics computations. We present and discuss results in section IV, while the final section concludes.

II. Potentials

The system studied in the present work is a model S_N2 reaction in water. The reaction examined here is $Cl^- + CH_3Cl$, which has been studied extensively by a number of groups both experimentally and theoretically in the gas phase and in aqueous solution.[1-7,9-12,32-51] In the gas phase, this system forms a stable ion-dipole complex at ~10 kcal/mol below the asymptotic (diatomic molecule and separated ion) limit.[2] The calculated gas-phase barrier to reaction,[2] as measured from the ion-dipole complex well, is 13.9 kcal/mol. Jorgensen and co-workers,[1,2] as well as Chiles and Rossky,[3] calculated the free energy profile of this reaction in water along the gas-phase reaction coordinate and found that the deep ion-dipole well almost completely disappears in solution. Instead, there is a very shallow well (on the order of 1 kcal/mol in depth, referred to the solvent-separated ion and the methyl chloride molecule), and an ~2 kcal/mol barrier to the breakup of this complex. (In the gas phase, there is no barrier to the formation of the ion-dipole complex from the separated reagents.) Also, the solution-phase free energy barrier to reaction, ~26 kcal/mol as measured from the ion-dipole complex, is considerably larger than the potential energy barrier in the gas phase. (The basic features of this free energy curve are consistent with the calculations of Warshel and co-workers,[6] who have used a different reaction coordinate based on their two-state model of this S_N2 reaction, the integral equation calculations of Huston, Rossky, and Zichi,[4] and the calculations treating the water solvent as a dielectric continuum by Tucker and Truhlar[42] and Kikuchi and co-workers.[43]) However, we stress that the previous computational studies[9,12] of the dynamics of this S_N2 reaction as well as the present calculations are not directed toward the determination of the mean potential; rather, as discussed in the introduction, they are focussed on examination of dynamics which may not, and typically do not, occur on the equilibrium free energy surface. What follows is a brief description of the different potentials used to model this S_N2 reaction in water. The paper of Bergsma et al.[9] contains more details as well as values for all the parameters used.

A. **$Cl^- + CH_3Cl$ Potential Energy Surface.** In their calculations, Jorgensen and co-workers[1,2] only took into account configurations lying along the one-dimensional collinear gas-phase reaction coordinate of the S_N2 system.[52] In order to carry out molecular dynamics for this system, as described by Bergsma et al.,[9] it is necessary to define the potential energy function for the other internal degrees of freedom. We simplify the system by treating the methyl group as a single united atom, thereby reducing the reagents to a triatomic system and the number of internal degrees of freedom to three. Following Bergsma et al.,[9] we use a LEPS potential energy function for the reagents. The parameters for the multidimensional LEPS surface are selected so as to reproduce approximately the one-dimensional gas-phase reaction coordinate behavior calculated by Jorgensen and co-workers.[2] In addition, since the asymptotic limit of the LEPS potential is a Morse potential for the methyl chloride molecule, those parameters that describe the Morse potential are chosen[9] so that the vibrational frequency of methyl chloride, 732.8 cm^{-1}, is approximately reproduced. The resulting gas-phase barrier height[9] is 13.9 kcal/mol measured with respect to the ion-dipole complex. The full list of parameter values is given by Bergsma et al.

More recently, Tucker and Truhlar[46,47] and Vande Linde and Hase[50] have separately performed very extensive ab initio electronic structure calculations on the gas-phase $Cl^- + CH_3Cl$ system and have performed a fit of the resulting energies to a functional form that takes into account all 18 degrees of freedom of this system. Potential functions such as these will allow examination of the effects of the methyl hydrogen "umbrella" motion[53] on this reaction that have not been readily accessible before. It is interesting to note that the LEPS potential energy function calculated by Tucker and Truhlar as part of their fit[47] shows many qualitative similarities to the LEPS potential used in previous[9-12] and the present simulations.

B. **Solvent Potential.** As in prior work from our laboratories,[9,12] the water potential of Watts[54] is used. This potential combines the intramolecular potential determined by Kuchitsu and Morino[55] with a semiempirical intermolecular potential. We use a full intramolecular potential (rather than rigid water molecules) which allows the water molecule to be flexible and all internal degrees of freedom to be included in the calculations. We thereby do not preclude the possibility of energy flow into and out of solvent vibrational modes. The intermolecular water-water potential is calculated as a sum of atom-atom interactions. The O-O interaction includes both a Coulomb and exponential repulsion as well as an attractive dispersion contribution. The latter contribution is meant to represent the dispersion potential for the entire bimolecular water-water interaction, but, for the sake of convenience, this interaction is associated only with the O-O interaction.[54]

The H-H interaction is taken to consist solely of repulsive Coulomb and exponential terms. The exponential part of this interaction is relatively small.

The O-H intermolecular interaction is particularly important in water because of the strong hydrogen bonding that takes place. Watts[54] found that the combination of an attractive Coulomb term plus a repulsive exponential term is insufficient to reproduce the known properties of water. To correct this, he supplemented the exponential term with a Morse potential. This extra "hydrogen bond" character results in a better fit to the experimental properties of water.[54]

For our purposes, an important feature of the Watts potential is that it contains parameters describing the hydrogen-bonding and Coulomb interactions between water molecules. We therefore expect that the effect of the solvent structure on the reagents will be well described by this potential. In addition, MD simulations by Berens et al.[56] show that this water model gives quite good agreement with the experimental heat capacity when quantum corrections are applied and has a heat capacity that is approximately 25% higher than experiment for purely classical simulations.

C. **Solvent-Reagent Potential.** The water solvent-S_N2 reagent interaction consists of two parts: Lennard-Jones interactions and Coulomb interactions between the charges on the reagent atoms and the charges on the atoms of the water molecules. The Lennard-Jones parameters of the reacting atoms are not allowed to vary with reaction coordinate (although in principle that could be done). The parameters of the Lennard-Jones interaction between given solvent and reagent atoms are calculated by using standard combining rules; the values of the appropriate parameters are given in Bergsma et al.[9]

In order to determine the Coulomb interaction between the reacting species and the water molecules, it is necessary to define charge distributions for the molecules, which we model as fractional point charges on the appropriate atoms. The use of such charges on the S_N2 reagent atoms and on the atoms of the water molecules, in addition to providing the necessary long-range forces for this system, mimics the hydrogen bonding between the solvent and reagent atoms through purely electrostatic interactions. This important point should be borne in mind when we refer in the future to the Coulombic interactions between the S_N2 reagents and the solvent water molecules.

For an individual water molecule, appropriate fractional charges are placed on the individual atoms such that the experimental dipole moment is reproduced and the entire molecule is electrically neutral. This process

---

(32) Morokuma, K. *J. Am. Chem. Soc.* **1982**, *104*, 3733.

(33) Carrion, F.; Dewar, M. J. S. *J. Am. Chem. Soc.* **1984**, *106*, 3531.

(34) Tanaka, K.; Mackay, G. I.; Payzant, J. D.; Bohme, D. K. *Can. J. Chem.* **1976**, *54*, 1643.

(35) Olmstead, W. M.; Brauman, J. I. *J. Am. Chem. Soc.* **1977**, *99*, 4219.

(36) Pellerite, M. J.; Brauman, J. I. *J. Am. Chem. Soc.* **1983**, *105*, 2672.

(37) Mitchell, D. J.; Schlegel, H. B.; Shaik, S. S.; Wolfe, S. *Can. J. Chem.* **1985**, *65*, 1642.

(38) Shaik, S. S. *Prog. Phys. Org. Chem.* **1985**, *15*, 197.

(39) German, E. D.; Kuznetsov, A. M. *J. Chem. Soc., Faraday Trans. 2* **1986**, *82*, 1885.

(40) Lee, S.; Hynes, J. T. *J. Chem. Phys.* **1988**, *88*, 6853.

(41) Lee, S.; Hynes, J. T. *J. Chem. Phys.* **1988**, *88*, 6863.

(42) Tucker, S. C.; Truhlar, D. G. *Chem. Phys. Lett.* **1989**, *157*, 164.

(43) Kozaki, T.; Morihashi, K.; Kikuchi, O. *J. Am. Chem. Soc.* **1989**, *111*, 1547.

(44) Van Doren, J. M.; DePuy, C. H.; Bierbaum, V. M. *J. Phys. Chem.* **1989**, *93*, 1130.

(45) Vande Linde, S. R.; Hase, W. L. *J. Am. Chem. Soc.* **1989**, *111*, 2349.

(46) Tucker, S. C.; Truhlar, D. G. *J. Phys. Chem.* **1989**, *93*, 8138.

(47) Tucker, S. C.; Truhlar, D. G. *J. Am. Chem. Soc.* **1990**, *112*, 3338.

(48) Tucker, S. C.; Truhlar, D. G. *J. Am. Chem. Soc.* **1990**, *112*, 3347.

(49) Benjamin, I.; Liu, A.; Wilson, K. R.; Levine, R. D. *J. Phys. Chem.* **1990**, *94*, 3937.

(50) Vande Linde, S. R.; Hase, W. L. *J. Phys. Chem.* **1990**, *94*, 2778.

(51) However, there has been to date no direct experimental measurement of the rate of this reaction in aqueous solution, although related reactions have been examined (cf.: Bathgate, R. H.; Moelwyn-Hughes, E. A. *J. Chem. Soc.* **1959**, 2642).

(52) Note that in solution, the most probable bend angle of the S_N2 reagent atoms in the model system at the transition state may not be collinear.[9,49]

(53) Ishida, K.; Morokuma, K.; Kormonicki, A. *J. Chem. Phys.* **1977**, *66*, 2153.

(54) Watts, R. O. *Chem. Phys.* **1977**, *26*, 367.

(55) Kuchitsu, K.; Morino, Y. *Bull. Chem. Soc. Jpn.* **1965**, *38*, 814.

(56) Berens, P. H.; Mackay, D. H. J.; White, G. M.; Wilson, K. R. *J. Chem. Phys.* **1983**, *79*, 2375.

gives a charge of −0.66 on the oxygen atom and +0.33 on each of the hydrogen atoms. In the simulation, the dipole moments (and all other multipole moments) of the water molecules dynamically change as the molecules vibrate.

For the $Cl^- + CH_3Cl$ heavy-particle charge-transfer system, a critical feature[9] of the reaction is that the charge distribution among the reagents shifts extensively as the reaction proceeds from the reagent ion–dipole complex to the transition state to the product ion–dipole complex. Thus, the fractional charge on each atom must be varied as a function of reaction coordinate, so that during the course of the reaction the negative charge switches smoothly from one chlorine atom to the other.[1,2] (Recall that the methyl group is approximated as a united atom.) To accomplish this, Bergsma et al.[9] define a charge switching function as a function of the quantity $r^2_{AB} - r^2_{BC}$, where the two distances are the two CH_3–Cl distances. (The charge switching is modeled after that of Jorgensen and co-workers which in turn is based on the interactions of the reacting species with a water molecule rather than on the gas-phase ab initio calculations.[2]) Note that the charge distribution on the reacting species in fact consists of point (rather than distributed) charges on each of the atoms; it is the magnitude of those charges that is controlled by the charge switching function. The sum of the fractional charges is of course always −1, the (unit) charge of an electron. As before, the parameters and the form of the charge switching function are given by Bergsma et al.[9] Note that in this model system, we do not take into account any direct polarization[5-7] of the solute by the solvent (although "charge shift" forces are accounted for[9,12]).

With the potential energy function defined, the force on any atom can be calculated as the its negative gradient. One must be careful to include the important effects of the variation of the charge on the reacting species in this calculation, but the method is otherwise fairly straightforward (Bergsma et al.,[9] Appendix A). With the forces in hand, the molecular dynamics calculations are comparatively simple, albeit computationally most intensive.

III. Molecular Dynamics Calculations

The molecular dynamics calculations are performed by integrating the classical Hamilton's equations of motion for the entire system. This is accomplished by using the leapfrog Verlet algorithm.[57] We perform calculations for a system containing the reagents and 256 water molecules by using a time step of 0.5 fs. This time step leads to a standard deviation in the total energy of ~0.01%. (Energy conservation improves as a smaller time step is used, but at the cost of significantly longer calculations.) We believe that the time step used here gives a good balance between the overall accuracy of the calculation and the computer time required.

A. Boundary Conditions. Our simulations use periodic boundary conditions in order to minimize edge effects. The "unit cell" used here is the periodic truncated octahedron.[58] This cell is space-filling and, because it is closer to being spherical than is a cubic unit cell, should better represent the spatial isotropy of a real liquid.

As is almost always the case with periodic boundary conditions, it is necessary to perform some type of potential truncation or summation over periodic images in order to make the calculation of the forces manageable. Here we use a minimum image convention[57] to define which molecules exert forces on a particular molecule at a given iteration of the molecular dynamics. However, we modify this by "feathering" or smoothly ramping the forces to zero as we approach the size of the unit cell. This approach avoids problems with spurious discontinuous forces at the boundary of the unit cell which might otherwise be quite large for the long-range Coulomb forces in the simulation. Note that we treat the existence of long-range forces solely by this feathering procedure; we do not use Ewald sums or other techniques for calculating the effects of all the images. (For a discussion of these alternative methods, see ref 57, Chapter 5.)

B. Preparation of Initial Conditions. In order to calculate a molecular dynamics trajectory, a set of initial conditions of the system must be specified, consisting of a set of positions and velocities for all atoms in the system. Choosing velocities for a system from the fixed temperature canonical ensemble is quite straightforward—one simply samples for all degrees of freedom from the Maxwell–Boltzmann distribution at the appropriate temperature. However, the choice of an initial configuration, i.e., a set of atomic positions, for the S_N2 system studied here is complicated by the high potential energy barrier to reaction as well as the persistent spatial correlations caused by the strong coupling nature of this system.

The general question of computationally sampling rare events, such as passage over a high barrier, has been dealt with by a number of authors.[9,12,19,59-65] In order to sample these events, the trajectories must be started from the top of the barrier and then integrated forward and backward in time. For the S_N2 system, we therefore require initial configurations with the reaction coordinate restricted to its value at the transition state (that is, the value of the asymmetric stretch of the $ClCH_3Cl$ system is zero[9,12]), while the values of all other degrees of freedom are chosen from the appropriate canonical ensemble.

For weak coupling systems, independent sets of initial configurations can be calculated simply from time evolution with the appropriate constraint on the reaction coordinate.[18-20] In the strong coupling system under consideration here, time evolution for computationally practical time spans may not be sufficient to guarantee independent initial configurations because spatial correlations may persist for long times. Therefore, as in a previous effort,[12] we create several independent seeds from each of which time evolution can be used to generate a set of initial configurations. This method assures a greater degree of independence than time evolution alone would provide.

Bergsma et al.[9] and Gertner et al.[12] have employed a unit cell containing the reagents plus 64 water molecules. This number of solvent molecules, which is almost two complete shells surrounding the reagents, was sufficient to understand the behavior of the reaction near the transition state—the main focus of the earlier work. However, the longer time and larger distance effects that we wish to study here require a larger number of solvent molecules.[66] Thus, we use a unit cell consisting of the reagents and 256 water molecules. This system contains essentially three complete shells of water molecules around the reagents. There is however a price to be paid. We find that building independent 256 water molecule systems from scratch, by using the technique Gertner et al.[12] employed for the 64 water case, is exceedingly difficult. We have therefore developed a new method for "bootstrapping" the larger system from sets of the 64 water system originally used by Gertner et al.[12] This method is presented in the Appendix.

By performing the tessellation procedure described in the Appendix for each of 10 seeds, i.e., independently created initial condition files, each containing 64 water molecules, we obtain 10 independent sets of equilibrated 256 water molecule systems. In these sets, the system of S_N2 reagents plus water molecules is sampled from the transition state. In other words, the asymmetric stretch of the reagents is set equal to zero, while the values of the other degrees of freedom of the reagents (the symmetric stretch and bend) and all the coordinates of the atoms of the solvent are chosen[12] from a canonical ensemble at 298 K. A process of repeated velocity randomizations and constant temperature dynamics is then used to generate several hundred sets of initial conditions (as described in the Appendix for the smaller system). These are generated from the 10 independently created seeds by performing 5 ps of equilibration with velocity randomizations every 250 fs to generate each set of initial conditions, with the starting point for each equilibration being the end of the previous equilibration. During this entire process, the asymmetric stretch of the reagents and the conjugate velocity are constrained to be zero.[67] From our original set of 10 independently created

---

(57) Allen, M. P.; Tildesley, D. J. *Computer Simulation of Liquids*; Clarendon Press: Oxford, 1987.

(58) Adams, D. J. In *The Problem of Long-Range Forces in the Computer Simulation of Condensed Media*; Ceperly, D., Ed.; National Resource for Computation in Chemistry: Berkeley, 1980; p 13.

(59) Keck, J. C. *Discuss. Faraday Soc.* **1962**, *33*, 173.

(60) Anderson, J. B. *J. Chem. Phys.* **1973**, *58*, 4684.

(61) Bennett, C. H. In *Algorithms for Chemical Computations*: *ACS Symposium Series 46*; Christofferson, R. E., Ed.; American Chemical Society: Washington, DC, 1977; p 63.

(62) Montgomery, J. S., Jr.; Chandler, D.; Berne, B. J. *J. Chem. Phys.* **1979**, *70*, 4056.

(63) Rosenberg, R. O.; Berne, B. J.; Chandler, D. *Chem. Phys. Lett.* **1980**, *75*, 162.

(64) Zichi, D. A.; Ciccotti, G. Hynes, J. T.; Ferrario, M. *J. Phys. Chem.* **1989**, *93*, 6261.

(65) Carter, E. A.; Ciccotti, G.; Hynes, J. T.; Kapral, R. *Chem. Phys. Lett.* **1989**, *156*, 472.

(66) In comparing results for the S_N2 system using both 64 and 256 water molecules, we have found that the short time (<100 fs) behavior described in ref 9–12 is essentially unaltered. However, at longer times, the amount of vibrational energy present in the reagents is considerably less for the 64 water molecule solvent than for the 256 water molecule solvent. A small number of trajectories with a solvent consisting of the 512 water molecule were also calculated, and those results did not show significant differences from the 256 water molecule system. Apparently, boundary effects due to the unit cell in the 64 water molecule case begin to have some spurious effects on the system at the longer times of interest in the present study.

seeds (equilibrated 256 water molecule systems), we thereby obtain a total of 210 sets of initial conditions.

C. **Trajectory Calculations.** Given an initial condition file specifying the position of all atoms, we calculate a trajectory by using molecular dynamics as follows. The constraint on the asymmetric stretch of the reagents is released. The velocities of all the atoms are chosen from a Maxwell–Boltzmann distribution, and the equations of motion are integrated both forward and backward in time to trace out a complete trajectory of approach to and recession from the transition state. Note that each individual trajectory is microcanonical (the total energy of the system is constant) but that the initial conditions are chosen from a canonical ensemble. As in the previous work,[9,12] one can then determine whether the trajectory is reactive. A reactive trajectory is defined by the reagents being on the reactant side of the barrier at large negative times and the product side of the barrier at large positive times. As has been shown[9,12] for the S_N2 reagents in water, all trajectories have their fate determined (in regard to being reactive or nonreactive) within ±50 fs of the reagents being at the transition state. However, in that ±50 fs, the reagents can cross the transition state more than once. The number of recrossings of the transition state that take place can be determined by examination of the value of the reaction coordinate for each trajectory as a function of time. The trajectories can then be analyzed based on the number of recrossings as well as their character as reactive or nonreactive events. Further analyses of special interest here, such as the monitoring of various potential and kinetic energies in the reagents and solvent, can be performed since all the positions, velocities, and forces are known at each time step.

Since we are primarily interested here in how the reagents climb the barrier and react, the majority of the results presented in the next section come from the analysis of the subset of trajectories that are reactive events. We have obtained 100 reactive trajectories. In order to obtain these, we calculate 1 ps of dynamics (500 fs on either side of the barrier) for 210 different sets of initial conditions. Each trajectory requires 100 CPU minutes on one processor of a four processor Silicon Graphics IRIS 4D/240GTX computer. In order to take advantage of the multiple processors, four separate trajectories (many trajectories are necessary in order to obtain good statistics) can be obtained by simultaneously using the four different processors with virtually no interference or performance degradation. Our throughput is thereby significantly enhanced. (For this type of computation, we obtain the equivalent of approximately 80 VAX 11/780 CPUs when all four processors are employed on an otherwise quiescent machine.)

IV. Results

In this work we will only discuss those trajectories that are reactive, that is, there is a net transition $Cl^- + CH_3Cl \rightarrow ClCH_3 + Cl^-$. Most of these trajectories cross the transition-state surface only once. (There are only four reactive trajectories that cross three times, the most we have seen in our work, but these do not show any significant differences with respect to energy flow, when considered as a class, from those that cross only once.) Most of our discussion will be from the perspective in which the reactants begin in the solvated ion–dipole complex $[Cl^-CH_3Cl]$ and climb the barrier to the transition state $[Cl^{\delta-}CH_3^{\delta+}Cl^{\delta-}]$ where they then cross the transition-state surface and go on to form products.

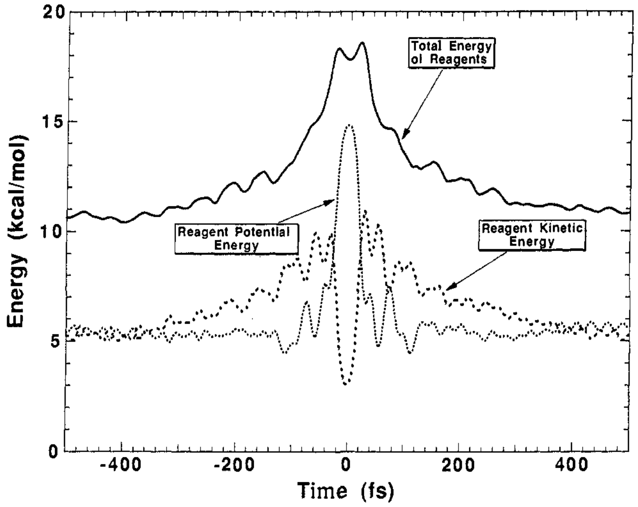

Figure 1. Kinetic, potential, and total energies in kcal/mol of the reagent atoms for the S_N2 reaction in water as a function of time. The time $t = 0$ is set to be at the top of the barrier to reaction (asymmetric stretch of the reagents equal to zero). The potential energy is referenced to zero at the gas-phase ion–dipole well. The energies are averaged over 100 reactive trajectories.

A. **Overview.** Since we are concerned with how energy flows from the solvent into the reagents and thereby drives the reagents up the barrier to reaction, it is useful to specify the types of energy that exist in the system. For each trajectory, the total energy of the system (reagents plus solvent) remains constant. The problem then becomes the division of this total energy among the various parts of our system. There are two obvious types of energy: kinetic and potential. We can further divide the kinetic energy into that for the solvent and that for the reagents. (The kinetic energy of the reagents could in turn be divided into that of vibration, rotation, and center of mass translation, as is discussed elsewhere.[9])

There are a number of different types of potential energies in this system, all of which are defined in section II. We summarize them as the following: intermolecular solvent potential energy, intramolecular solvent potential energy, solvent–reagent potential energy, and reagent potential energy. We monitor all of these for each molecular dynamics trajectory. In the figures below, we will display each of these energies as a function of time with $t = 0$ denoting the time at which the reagents are at the transition state. (Since we are primarily interested in the qualitative behavior of these quantities, we have not performed a detailed error analysis.[12] However, because our trajectories are independent, a reasonable estimate of the relative error in our averages is $\pm 1/(\text{number of trajectories})^{1/2}$ or ±10% for the ensemble of 100 reactive trajectories calculated here.)

In Figure 1, we present the potential and kinetic energies of the S_N2 reagents as well as their sum for our ensemble of reactive trajectories. Note that the symmetry between ascent and descent of the barrier is clearly reflected in the symmetry between positive and negative times apparent in this and subsequent figures. The first feature of Figure 1 that we wish to point out is the behavior of the reagent energy at different times. At times prior to −350 fs, the total energy of the reactants is essentially constant,[68] with the energy evenly divided between potential and kinetic energy. (As we shall discuss later, the vibration of the methyl chloride is not at all thermalized within the ±500 fs shown; instead, it has been activated before $t \sim -500$ fs to an average vibrational energy of 10 kcal/mol corresponding to $v = 5$ and produced in this state at $t \sim 500$ fs.) At about −350 fs, energy begins to flow from the solvent into the reactants. The kinetic energy of the reactants begins to increase, and this steady increase continues until approximately −50 fs. During most of this phase, their potential

---

(67) As Carter et al.[65] have discussed, the appropriate ensemble of initial conditions is that in which the value of the asymmetric stretch is restricted to be zero but not constrained to that value. However, initial configurations are most readily generated by using algorithms in which the asymmetric stretch is constrained to be zero. Carter et al.[65] have described a general method for correcting for the use of the constrained ensemble. The correction factor for a constraint on the asymmetric stretch of the S_N2 reagents is related to the asymmetric stretch mass μ_{as}

$$\mu_{as} = 2/[1/m_{Cl} + 1/m_{CH_3}(1 - \cos\theta)]$$

where θ is the bend angle of the reagents. If μ_{as} were constant with respect to θ, the results of the constrained ensemble would be equal to that of the restricted ensemble. In the S_N2 system studied here, the average value of μ_{as} is less than 1% greater than its collinear value. Thus, the effect of correcting for use of the constrained ensemble is extremely small for the results discussed in section IV. This formula for μ_{as} differs from an incorrect one given in eq 3.9 of ref 12. The expression in that reference agrees with the one here for collinear geometries, and the average values of the expressions over the set of initial conditions do not differ by more than 2–3% in the most extreme case. Thus, the results of that work that involve the use of the asymmetric stretch mass would be changed by an amount that falls well within the error bars of those results.

(68) We have verified that this approximately constant energy in the reagents holds to at least 1 ps away from the transition state through calculation of 20 trajectories for ±1 ps on either side of the transition state.

transition state.[73] This discussion has been couched primarily in structural terms and therefore does not give much sense of the underlying dynamical processes governing these energy changes. In the remainder of this section, we discuss the processes by which these energies evolve as well as their time scales in order to gain a deeper insight into the mechanism of this S_N2 reaction.

B. Reagent Dynamics. Figure 1 has displayed the energies of the S_N2 reagents. In order to understand further the influence of the solvent on these energies, we now consider two modifications of our model system. First, in Figure 3a, we determine the reagent energies for a set of 20 gas-phase, i.e., isolated reagent, trajectories in order to highlight the overall effect of the solvent. The initial positions of the reagent atoms are chosen to be the same as for a randomly selected set of trajectories in the water solvent, while the initial velocities are again chosen from a Maxwell–Boltzmann distribution. Second, in Figure 3b, we display the results of 20 trajectories for which the charges on the S_N2 reagent atoms are set to zero, thereby turning off the long-range Coulomb interaction between reagents and the water solvent. The initial conditions for these trajectories are computed from the equilibration process described in the Appendix but now for the system with charges on the reagents turned off.

The internal dynamics of the isolated S_N2 reagents, as shown in Figure 3a, display significant differences from their dynamics in the water solvent (a point established in previous work[9]). This is the key point. Nonetheless, there is one important similarity: the time scale for the climbing of the barrier is approximately 50 fs in both cases. The consonance of these time scales indicates that during the 50 fs before the transition state is reached, the gas-phase forces (that is, the reagent internal forces) dominate the reagent dynamics with the overall effect of the solvent being only a small perturbation.[74] However, the vast difference in the internal S_N2 dynamics between isolated reagent and solution behavior during the remaining time span apparent in Figures 1 and 3 underscores the importance of the water solvent for the overall reaction process.

But the mere presence of solvent molecules is insufficient to duplicate the internal S_N2 dynamics of Figure 1. Figure 3b displays the internal dynamics of the S_N2 reagents in water but now with no charges on the reagent atoms. (The potential energy functions for the interactions of the reagent atoms among themselves and the solvent atoms among themselves are left unaltered.) Here we see that the dynamics are very much closer to that of the isolated S_N2 system than to that of the reagents in water with all charges turned on. In particular, the total energy of the reagents remains almost constant over the entire time span examined. The strong interaction between the reagents and solvent due to the Coulomb interaction clearly plays a major role in determining the course of the reaction dynamics.

C. Solvent Effects: Potential and Kinetic Energies. Having demonstrated the importance of the water solvent in producing the observed set of reagent dynamics, we can now turn to understanding how the solvent affects the overall S_N2 reaction dynamics. We begin this endeavor by examining global properties of the solvent. In Figure 4, we dissect the total energy of the water displayed in Figure 2 into intermolecular potential, intramolecular (vibrational) potential, and kinetic energy terms.

As discussed in section II.A, the total energy of the S_N2 reactants must increase on average by ~7 kcal/mol over the 500 fs time span examined here for them to reach the top of the barrier. Because the entire system (reagents plus solvent) in any given trajectory has a constant energy, this increase in reagent energy must be reflected by decreases in some or all of the other types of energy in the system. The intramolecular potential energy of the water molecules remains constant (aside from thermal fluctuations) over the course of the reaction. This result implies that the intramolecular, high-frequency vibrations of the water molecules do not directly contribute any of the energy required to drive the reactants up the barrier. Insofar as the reaction is concerned, these vibrations are spectators.

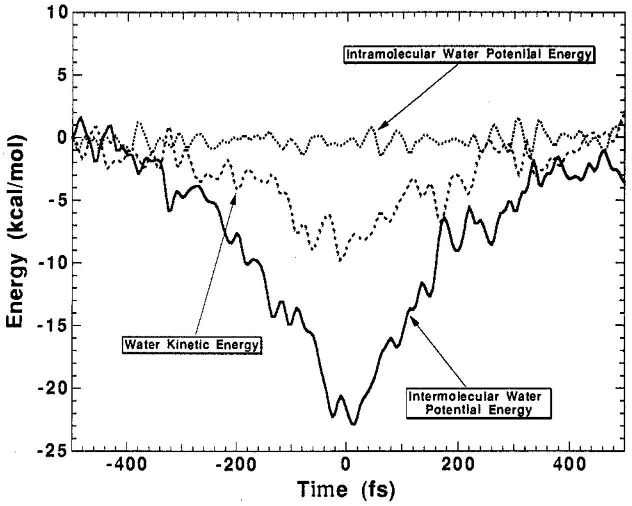

Figure 4. Energies in kcal/mol of the water solvent as a function of time: intermolecular potential energy of the solvent, kinetic energy of the solvent, and intramolecular potential energy of the solvent. These quantities are averaged over 100 reactive trajectories, and the data have been smoothed prior to display. All energies are referenced to their values at −500 fs.

The energy fueling the ascent of the reagents up the potential energy barrier, in fact, comes primarily from the intermolecular water solvent potential energy which contributes approximately 19 kcal/mol (see Figure 4). The water solvent kinetic energy is however by no means a completely silent partner; it also contributes a significant amount of energy (on the order of 9 kcal/mol). There is another key aspect revealed by Figure 4: The total energy that the solvent loses during the course of the attainment of the transition state goes to the solvent–reagent interaction potential energy as well as to the total energy of the S_N2 reagents (as is evident from Figure 2).

The potential energy of the solvent thus contributes twice as much energy as the solvent kinetic energy. This result stands in complete contrast to the weak coupling case in which the rare gas solvent contributes energy primarily through impulsive collisions leading to transfer of kinetic energy.[20] In that case, the predominance of solvent kinetic energy over potential energy contributions was understood through an analysis of the heat capacity of the rare gas solvent. For ease of discussion of this weak coupling case, we focus here on the perspective in which the reagents come off the barrier toward products. Since the strong forces of the reagent–solvent interaction in the weak coupling case extend only over a very short range, the energy that the reaction system loses as it comes off the barrier is transferred very quickly to the rare gas solvent through impulsive collisions. The excess energy is then collisionally dissipated through a few solvent molecules where it shows up in both kinetic and interatomic potential energy of the solvent. This energy transfer can be thought of as a localized "heating" of the solvent. Benjamin et al.[20] have shown that the ratio of the increase in kinetic energy to the increase in potential energy can be related to the constant volume heat capacity C_V of the system and, equivalently, to the temperature fluctuations of the system. By determining the temperature fluctuations from molecular dynamics calculations, they find[20] for a model Cl + Cl_2 reaction in a liquid Ar solvent[19] (where the solvent is weakly coupled to the reagents) that the heat capacity arguments give $\Delta V/\Delta K = 0.43$, where ΔV is the change in potential and ΔK is the change in kinetic energy of the Ar solvent. This result is in good agreement with the MD results[20] for this quantity.

---

(73) Because we release the energy stored at the barrier top into a finite number of water molecules in our microcanonical trajectories, there is an excess of energy at times before and after $t = 0$ compared to what would be expected if an effectively infinite external heat bath were able to provide and carry off energy. The result is an increase in the temperature of the system over the 298 K at the barrier top where the initial velocities are chosen. However, this 9 kcal/mol increase in the kinetic energy of the solvent only leads to an ~3 K temperature increase for the 256 water molecule system. This small rise in temperature should have no appreciable effect on the results presented here.

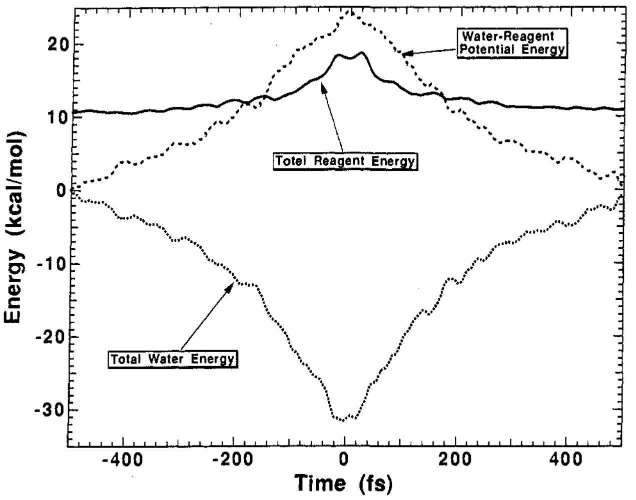

Figure 2. Energies in kcal/mol of the S_N2 system in solution as a function of time: potential energy of the S_N2 reagents, potential energy of interaction between the solvent and reagents, and total energy (intermolecular potential + intramolecular potential + kinetic energy) of the water solvent. These energies are averaged over 100 reactive trajectories. The total water energy and the solvent–reagent interaction energy are referenced to their values at −500 fs.

energy remains roughly constant, but betwen −100 and −50 fs it also begins to increase dramatically. Finally, in the last 50 fs before the system reaches the transition state, the reactant kinetic energy drops precipitously, the reactant potential energy increases rapidly, and the system reaches the top of the potential energy barrier posthaste. Over the barrier-climbing process, the total energy of the reactants increases from an average of ~11 kcal/mol at $t = -500$ fs to ~18 kcal/mol at the top of the barrier. This 7 kcal/mol difference represents the amount of energy over and above the energy already present in methyl chloride vibration that the solvent must put into the reactants for the climb of the barrier to take place. The S_N2 reagents' energy at $t = 0$ of 18 kcal/mol is of course somewhat higher than the 13.9 kcal/mol that the reagents would need to just reach the top of the potential energy barrier. The total energy of the S_N2 reagents at the transition state includes not only that of the potential energy barrier but also a thermal distribution of energy in all degrees of freedom of the reagents other than the reaction coordinate. This point should be remembered in the discussion below concerning energy flow into and out of the S_N2 reagents.

We now turn to the water solvent energetics and display the solvent–reagent interaction energy and the total water energy as a function of time in Figure 2 along with the reagent potential energy. Figure 2 shows that the total energy of the water molecules steadily decreases (becomes more negative) over the 500 fs time span up to $t = 0$. In addition, there is a steady increase in the solvent–reagent interaction energy over the course of the barrier-climbing process.

Thus, in the −500 to 0 fs time frame, the energy lost over the course of the barrier-climbing process by the water solvent potential and kinetic energies does *not* go mainly into the reactants. A much larger amount (on the order of 22 kcal/mol) shows up as an increase in the solvent–reagent potential energy.

This increase in the unfavorability of the solvent–reagent interaction can be understood as a difference in the solvation at the bottom of the barrier from that at the transition state. At the bottom of the barrier, the reagents are in an ion–dipole complex $[Cl^-CH_3Cl]$. The solvation of this complex is dominated by the favorable solvation of the chloride anion. At the top of the barrier, however, the reagents have a symmetric charge distribution $[Cl^{\delta-}CH_3{}^{\delta+}Cl^{\delta-}]$ with the negative charge of the complex spread out evenly over the two chlorine atoms. The solvation of this complex will be weaker than that of the charge localized chloride ion. Thus, as the system changes from the charge localized ion–dipole complex to a symmetric charge distribution in climbing the barrier, the solvent–reagent interaction potential energy will increase due to the decrease in the effectiveness of the solvation of the negative charge. Concomitantly, the intermolecular water potential energy decreases, that is, become more negative. (Note the decrease in the total solvent energy in Figure 2.) The diminished solvation of the reaction complex allows the water molecules to interact more favorably with each other rather than being unfavorably positioned in the process of solvating the chloride anion. These calculations confirm computationally the notion of differential solvation for reactants and transition states long familiar in the physical organic literature.[69–72]

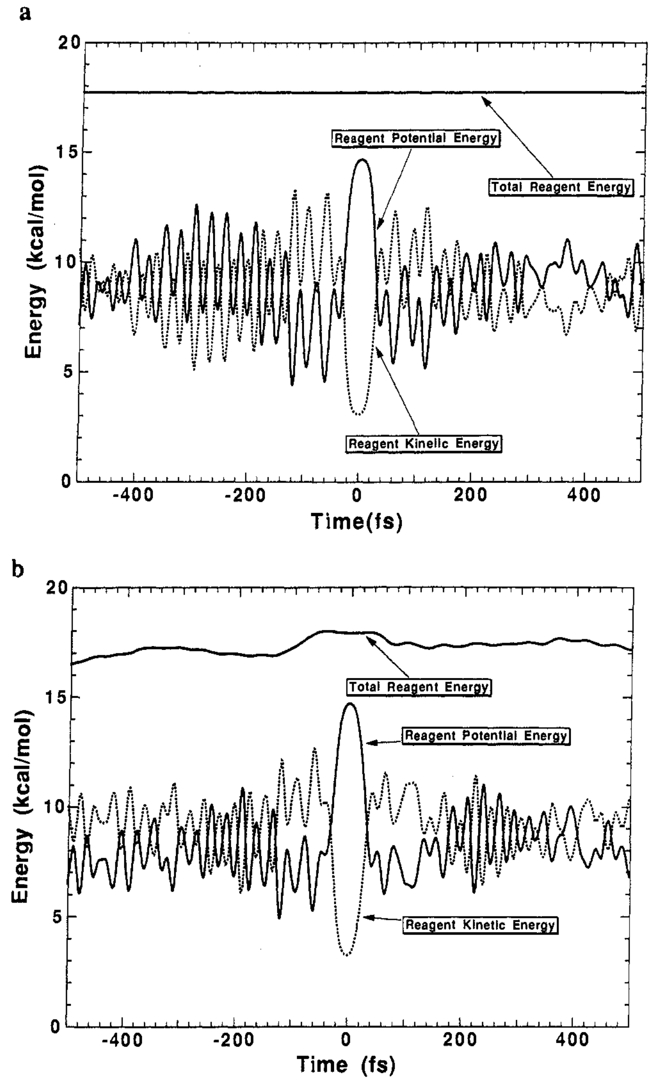

Figure 3. (a) Same as Figure 1 except for the gas-phase S_N2 reaction and (b) same as Figure 1 but with no Coulomb interaction between the S_N2 reagents and the water solvent. All results are averaged over 20 trajectories.

This discussion establishes a central point. The solvent plays two distinct roles in the ascent to the transition state. The first, portrayed in Figure 1, is to transfer energy to the S_N2 reagents. The second, depicted in Figure 2, is to reorganize itself with a concomitant considerable increase in the solvent–reagent potential energy. These two roles should be kept in mind in the ensuing discussion.

We have explained here how the values of the various types of energy in this reaction in solution differ from the values at the

---

(69) Ingold, C. K. *Structure and Mechanism in Organic Chemistry*; Cornell University: Ithaca, 1969.

(70) Parker, A. J. *Chem. Rev.* **1969**, *69*, 1.

(71) Lowry, T. H.; Richardson, K. S. *Mechanism and Theory in Organic Chemistry*, 3rd ed.; Harper and Row: New York, 1987.

(72) Reichardt, C. S. *Solvent Effects in Organic Chemistry*; Verlag Chemie: Weinheim, 1979.

For the present aqueous S_N2 reaction, we expect that since the heat capacity of water is considerably larger than that of Ar at liquid densities, the relative potential energy contribution from the water solvent should also be much larger. However, in attempting to relate the heat capacity to the ratio of potential energy to kinetic energy contributions, we encounter a new problem. From the formulas in ref 20, we find

$$\frac{\Delta V}{\Delta K} = \frac{2C_V}{3Nk} - 1 \qquad (2)$$

where N is the number of atoms in the system and k is Boltzmann's constant. In contrast to the weak coupling case, there is a very strong interaction between the solvent and the reagents, as Figure 2 amply demonstrates. In order to appeal to heat capacity arguments, we must have a definition of ΔE in the relation $C_V = \Delta E/\Delta T$. One reasonable choice is to take ΔE to be the sum of the decrease in total energy of the reagents plus the loss of energy in the solvent–reagent interaction as the reaction comes down the barrier from the transition state. We use this interpretation of C_V here with the implication that the proper heat capacity to use in eq 2 is that of the pure solvent. Berens et al.[56] have calculated C_V for Watts water[54] by using molecular dynamics and obtained a value of 106.5 J/K mol. (This value is that for the classical solvent before application of the quantum corrections described in ref 56.) By using this value and eq 2, we find that $\Delta V/\Delta K = 1.85$. This value agrees reasonably well with that obtained from Figure 4 ($\Delta V/\Delta K \sim 2.1$).

The agreement of this simple calculation with the molecular dynamics results (in both weak and strong coupling systems) is important for two reasons. First, it gives a simple rule of thumb for determining the balance between the kinetic and potential energies in providing the energy necessary to climb the barrier to reaction (or, equivalently, to receive the energy when the reagents come off the barrier). Second, it highlights the different effects that the rare gas and water solvents have on the respective reagents in a barrier ascent. The rare gas solvent transfers its energy to the neutral reagents through impulsive collisions that transfer kinetic energy. For this to occur, a "hot spot" in the solvent must have developed at some earlier time resulting in some solvent atoms with high kinetic energy. In the aqueous S_N2 case, a different kind of priming of the solvent must take place. The energy transfer to the S_N2 reagents occurs primarily by way of the potential energy of the solvent. The fluctuation that develops in the solvent must therefore be of a qualitatively different type than that in the rare gas solvent. In the aqueous S_N2 reaction, the fluctuation occurs primarily on the coordinate side of phase space rather than on the momentum side as observed in the study of the weak coupling system.[20,30] One could therefore speak here of a "strain" rather than a hot spot. As we shall see presently, the processes that lead to the transfer of energy to the reagents are also quite different.

D. Solvent Effects: Work Done on the Reagents. Figure 1 has shown that there is a significant increase in the total energy of the reagents over the course of the climb to the transition state. We have shown in section II.C that this increase in total energy is accompanied by a decrease in the intermolecular solvent potential energy as well as the solvent kinetic energy. In other words, energy flows from the solvent to the reactants (and to the solvent–reagent interaction potential energy as well). In the remainder of this section, we will discuss in greater detail the nature of this energy flow during the barrier-climbing process. A useful quantity for examining this energy flow is the work done on the reagents by the solvent.[20] Ohmine[75] has previously examined this quantity in a study of the relaxation of ethylene vibration and internal rotation in water.

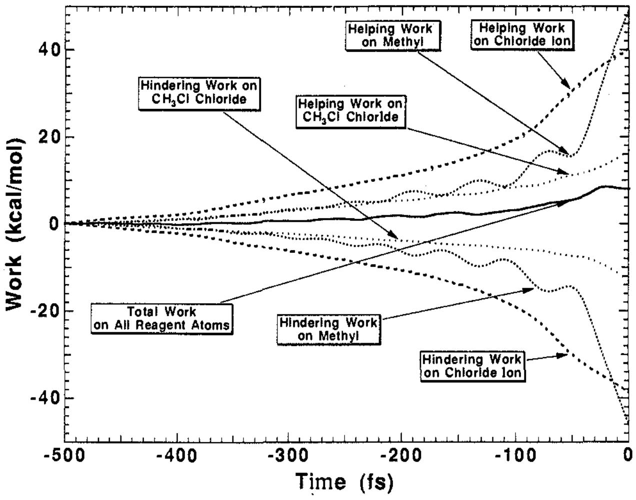

Figure 5. Helping and hindering work, in kcal/mol, exerted on each of the S_N2 reactant atoms by the water solvent as a function of time. The total work, which is the sum of all helping and hindering work on all the reactant atoms, is also displayed. These quantities are averaged over 100 reactive trajectories.

We define the work $W_{j\nu}(t)$ done by solvent molecule j on reagent atom ν up to time t by

$$W_{j\nu}(t) = \int_{t_0}^{t} \mathbf{F}_{j\nu}(\tau)\cdot\mathbf{v}_{\nu}(\tau)\,\mathrm{d}\tau \qquad (3)$$

where t_0 is a reference time (usually taken here to be −500 fs), $\mathbf{F}_{j\nu}$ is the force exerted on the reagent atom ν by the solvent molecule j, and $\mathbf{v}_\nu$ is the velocity of the reagent atom. The effect on the total energy E_r of the reagents is given by

$$E_r(t) - E_r(t_0) = \sum_{j,\nu} W_{j\nu}(t) \qquad (4)$$

Note that the reagent energy E_r does not include any potential energy of interaction with the solvent. Thus, we can account for the energy change of the S_N2 reagents by examining the work done on these atoms by all the water solvent molecules.

It is useful at this point to introduce the concepts of "helping" and "hindering" work. The work done by any particular solvent molecule on the reagents can be positive or negative. As eq 4 shows, positive work deposits energy into the reagents; negative work removes energy. We define helping work as that work which helps the reaction progress to completion; hindering work hinders that progress. For reactants climbing the barrier, it is positive work that deposits energy into the system and thereby is the helping work; negative work removes energy and hampers the barrier ascent. (However, after the reagents reach the transition state and begin to fall off the barrier, it is negative work that removes energy from the products and thereby assists the progress of the reaction.) The work done by any water solvent molecule on the S_N2 reagents can thus be classified as helping or hindering.

In Figure 5, we plot the total helping and hindering work on each S_N2 reactant atom as a function of time for the barrier-climbing process. We also display the total work summed over all reactant atoms. We first observe that there is a large amount of *both* helping and hindering work done on all three reactant atoms. In fact, the helping work done on any particular atom is much greater than the total work done on the reactants (~7 kcal/mol). These results reveal that there is a large cancellation between helping and hindering work. The net consequence is that enough energy is put into the reactants by the solvent so that the reactants can climb the reaction barrier, but the net amount of energy gained by the reactants does not reflect the underlying massive tug-of-war taking place in this process.

Figure 5 also indicates which atoms of the S_N2 reactants have what work done on them and at what time. We see that while the work is done predominantly on the chloride ion for most of the reaction, in the last 50 fs the majority of the work is done on

---

(74) Note that at the transition state, the internal forces of the reagents become very small and are in fact zero at the saddle point of the potential energy surface. Thus, the solvent effect on the reagents is crucial to understanding the reagent dynamics at the transition state. See, for example, the transition-state behavior calculated in previous simulations of this S_N2 reaction.[9-12]

(75) Ohmine, I. *J. Chem. Phys.* **1986**, *85*, 3342.

the methyl group. The work done on the methyl group also shows an interesting oscillatory pattern in the time span between −350 and −50 fs. The frequency of these oscillations corresponds roughly to that of the methyl chloride vibrational frequency. Since we plot the ensemble average of the work in Figure 5, the increasing amplitude of these oscillations as $t \rightarrow 0$ likely represents the vibrations of the ensemble of methyl chloride molecules coherently coming into phase as the top of the barrier is approached.

We wish to stress again the strong effect that the solvent has on the reagent atoms as evident in the large amount of both helping and hindering work done on these atoms. This result is very different from what happens in the weak coupling system: there helping work is clearly dominant, and the total work is nearly equal to this helping work.[20] In the present strong coupling system, the solvent both helps and hinders the progress of the reaction in a significant manner. The end result of this tug-of-war is that just enough energy to drive the reagents up the barrier is provided by the solvent.

With these results in hand, we can describe in somewhat greater detail how the time scales in Figure 1 arise. First, at times earlier than 350 fs from the transition state, we see that the solvent does not do much work on the reagents and the total energy of the S_N2 reagents is therefore approximately constant. However, the energy in the reagents is greater than what we would expect from a system in thermal equilibrium with its surroundings. We have determined that the excess energy is primarily contained in the vibration of the methyl chloride molecule and corresponds to an average energy of 10 kcal/mol or a vibrational level $v = 5$. Thus, the first process in the reaction is the vibrational activation of the methyl chloride at some time presumably significantly greater than 500 fs before the system reaches the transition state.[76]

During the second time scale, that from −350 to −50 fs, the situation is much more complicated. The work done on the methyl group begins to show oscillations in this time span, indicating some significant coupling between the vibration of the methyl chloride and the solvent forces acting upon it. (This coupling surely exists at earlier times, but the oscillations are washed out by vibrational phase incoherence in the ensemble average.) In addition, the chloride ion has a large amount of work done on it in this time span, indicating that a significant *net* interaction with the solvent has begun to take place.

In the final 50 fs, the reagents do most of the climbing of the barrier. The profile of the work done is quite different in this stage compared to the previous phases. We now see a very large amount of work being done on the methyl group with somewhat less work being done on the two chlorines. This result is perhaps initially surprising, given the relative magnitudes of the charges on the individual atoms. However, this behavior can be better understood by examining in detail the reaction coordinate for this process. In previous work,[9] a reaction coordinate, r_{as}, the asymmetric stretch noted in the previous section, has been defined by

$$r_{as} = \tfrac{1}{2}(r_{Cl'-CH_3} - r_{CH_3Cl}) \qquad (5)$$

r_{as} being zero at the transition state. From the discussion of charge switching given by Bergsma et al.[9] and summarized in section II.C, we see that in the region of the barrier top, the charge switching is strongly dependent on r_{as}. We can calculate the work done on r_{as} by the water solvent, and we display the results for the last 100 fs of the reaction process in Figure 6. For comparison, we also show the sum of the work done on all other degrees of freedom of the S_N2 reactants over this time span. Clearly, the vast majority of the total work done on the S_N2 reactants in the final 50 fs as the system climbs the barrier is done on this reaction coordinate. The light mass of the methyl group means that during this time span it will tend to move more than the more massive chlorine atoms (as it is transferred from one to the other) and therefore have more work done on it.[77] (In this limited sense, one could regard this S_N2 reaction as a methyl group transfer.[78]) As we shall see presently, this comparatively extensive motion of the methyl group over a short time leads also to a rapid change in the charge distribution. This swift movement of charge will be seen to have some important effects on the time scales of energy change in the solvent.

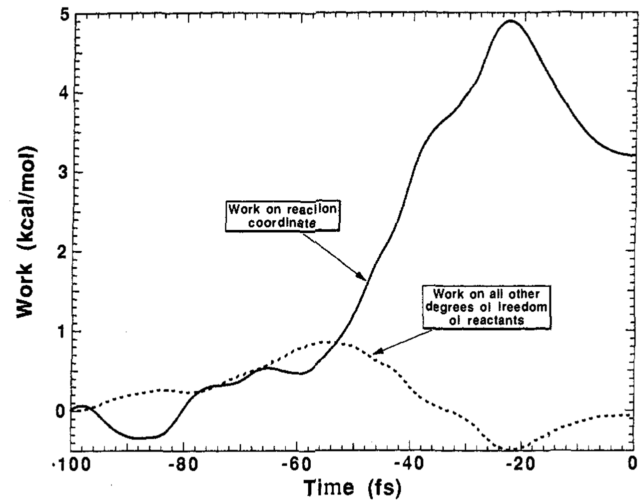

Figure 6. Work exerted by the water solvent, in kcal/mol, on the reaction coordinate as defined in eq 5 as well as total work on all other degrees of freedom of the S_N2 reagents as a function of time. Results averaged over 20 trajectories.

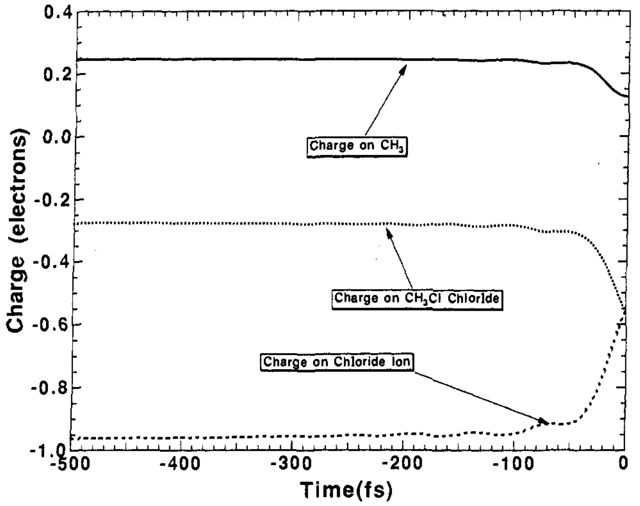

Figure 7. Charge in units of electrons on the S_N2 reagent atoms as a function of time. These quantities are averaged over 100 reactive trajectories. Note that even at ±500 fs, the charge on the chloride ion is not quite −1. This nonasymptotic value of the charge occurs because the average separation of the chloride ion and methyl chloride molecule at ±500 fs is smaller than that in the gas-phase ion–dipole complex due to the vibrational motion of the methyl chloride molecule.

E. Solvent Time Scales. In the previous sections, we have described in some detail the time scales that we have identified for the dynamics of the reaction. However, examination of Figure

---

(76) The existence of vibrational activation for the gas-phase $Cl^- + CH_3Cl$ reaction (as well as some non-RRKM behavior in the united atom approximation for the methyl group) was originally noted by Bergsma et al.[9] More recently, Vande Linde and Hase[45] have found for the dynamics of this reaction in the gas phase that the reaction is significantly promoted if the methyl chloride vibration is excited to the $v = 4$ state or above.

(77) We have confirmed that the mass of the methyl group is a determining factor in how much work is done on this united atom in the following manner. We have calculated 10 trajectories for each of the two additional systems where the mass of the methyl group is varied, but all other components of the system are identical with the system discussed in the text. In the first case, the methyl mass was set equal to 31 amu; in the second case, the methyl mass was set equal to 79 amu. (In the original trajectories, the methyl mass is 15 amu.) As the methyl mass increases, the amount of helping and hindering work done on the methyl group decreases substantially, becoming half as much in the case of the largest mass as in the original system.

(78) Albery, W. J.; Kreevoy, M. M. *Adv. Phys. Org. Chem.* **1978**, *16*, 87.

2 shows that during the 500 fs of the barrier-climbing process which we examine, there are at most two time scales that can be discerned from the water solvent energies (in contrast to the three time scales we have discussed for the S_N2 reagents). From Figure 2, we see that the changes in the solvent energy and the solvent–reagent interaction potential energy are gradual over most of the 500 fs time span. These smooth changes imply that the change in the solvation of the reaction complex is also smooth and gradual over this time period. But the change of the charge distribution in the reagents is not at all gradual over this 500 fs. In Figure 7, we plot the charges on the three reagent atoms as a function of time averaged over 100 reactive trajectories. The transition from ion–dipole to symmetric charge distribution occurs almost entirely over the last 50 fs before the system reaches the transition state. (This time scale[9] is in reasonable agreement with that seen by Warshel and co-workers[6] in their calculations where solvent and solute polarization are taken into account.)

These results indicate that a major portion of the reorganization of the solvent to a state appropriate to solvating the symmetric charge distribution of the reagents at the barrier top takes place *well before* the charge distribution on the reagents begins to change. The solvation cannot adiabatically follow the rapid change in the distribution of the negative charge among the reagents.[79] This prior solvent reorganization is *required* for the reagents to reach the transition state. This result is an extension of one from Bergsma et al.[9] where the outcome of the reaction for each trajectory and, in fact, the value of the transmission coefficient were found to be primarily determined by the relative solvation of the two chlorine atoms at the transition state.[10,11,40,41] We have now confirmed that this solvation at the transition state has begun to develop well before any change in the charge distribution in the reagents. Of related interest is the work of Maroncelli and Fleming[80] who have studied the response of water solvent to an instantaneous change in the charge of an ionic solute, of Simon, Haymet, and co-workers[81,82] who have studied the response of water to an instantaneous change in the dipole of a solute, of Warshel and co-workers[6,7] who have calculated the time scale of the solvent response for several charge-transfer reactions in water, including the present S_N2 reaction, and of Bader and Chandler[83] who have examined a similar response for Fe^{2+}–Fe^{3+} in water. The time scales that these groups find for the solvent relaxation under these conditions—and that originally found in refs 9 and 12 for the time-dependent friction on the S_N2 transition state—are similar to those we find for the prior reorganization of the solvent.

While the total energy of the water decreases for almost all of the reactive process, in the last 20 fs before the S_N2 reaction system reaches the transition state, the total water energy appears to remain approximately constant (cf. Figure 2). This result is consistent with the frozen solvent nonadiabatic solvation model developed earlier[9,10,12,15-17] to explain the transition-state dynamics of this system. By assuming with this model that the solvent molecules do not move significantly during this time interval, we can interpret the changes in the total energy of the reagents and the solvent–reagent interaction energy over this short time span (see Figures 1 and 2) as follows. (For the sake of exposition, we will develop this interpretation in terms of the reagents coming off the top of the barrier.) As the reagents come off the barrier ($Cl^{\delta-}CH_3^{\delta+}Cl^{\delta-} \rightarrow ClCH_3Cl^-$), the negative charge on the incipient chloride ion begins to increase, and the negative charge on the chlorine end of the incipient methyl chloride molecule begins to decrease. However, because there is also a variation in the (positive) charge on the methyl group, these chlorine charge changes are not symmetric (see Figure 7) with the chloride ion gaining more charge than the chlorine of the methyl chloride is losing. Thus, the overall effect will be strong attraction of the chloride ion to the water molecules that are hydrogen bonded to it. This attraction will tend to decrease (make more negative) the solvent–reagent potential energy, as we see from Figure 2. With our assumption that the solvent is frozen, this energy can only be channeled into the reagents, leaving the total solvent energy fixed. Since the potential energy of the reagents is decreasing smoothly (see Figure 1), the extra energy must end up as kinetic energy of the S_N2 reagent atoms, consistent with the idea[9] that the chloride ion is accelerated off the barrier by the electrostatic field created by the frozen solvent molecules. This picture of the short-time behavior of the reagents is also consistent with the two peaks in the total energy of the reagents seen in Figure 1. This entire process occurs in ~20 fs, at the end of which a large portion of the charge switching has taken place. In this picture, the solvent then begins to relax and readjust to the new charge distribution ($ClCH_3Cl^-$). The aqueous solvent is then able to remove energy from the reagents, thereby accounting for the beginning of the decrease in the reagent total energy that we see after 20 fs. (Note also that the reagent potential energy is still significantly changing after 20 fs, particularly in the time period up to 50 fs. In this period, *both* the reagent and solvent dynamics are important.[84]) Thus, the frozen solvent model gives a consistent and intuitively pleasing picture of the dynamics over the first 20 fs after the reagents leave the top of the barrier and is consistent with previous work on the reaction rates and recrossings of this system.[4,9,10,12,15-17,40,41]

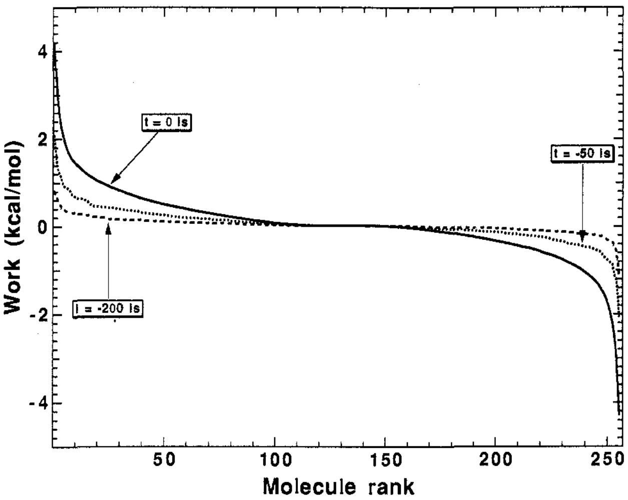

Figure 8. Total work done on the S_N2 reagents as a function of water solvent molecule rank. The solvent molecules are ranked on the basis of the total work done from −500 fs up to time t of the barrier-climbing process ($t = 0$ is set to be the time at which the reagents are at the top of the barrier). The total work is then displayed for $t = 0$, $t = -50$ fs, and $t = -200$ fs. These quantities are averaged over 100 reactive trajectories.

F. Many Molecule Solvent Effects. An important result from analysis of the weak coupling system was that relatively few solvent atoms are involved in transferring energy to the reagents in the barrier ascent.[20] The predominant mode of energy transfer was that of one or two impulsive collisions, each transferring a large amount of kinetic energy to the reagents.

The modes of energy transfer in the S_N2 reaction in water are quite different. We can see this most clearly by considering the work that each water solvent molecule j does on the S_N2 reagents. We define this quantity W_j by

$$W_j(t) = \sum_{\nu} W_{j\nu}(t) \tag{6}$$

in which the sum is over the three S_N2 reagent atoms. For each reactive trajectory, we determine $W_j(t)$ for each of the 256 solvent

---

[79] Of course, in the reactant and product wells, the reagent motion and solvent motion time scales can be comparable.

[80] Maroncelli, M. P.; Fleming, G. R. *J. Chem. Phys.* **1988**, *89*, 5044.

[81] Banet, M.; Karim, O. A.; Simon, J. D.; Haymet, A. D. *J. Nucl. Phys. B (Proc. Suppl.)* **1988**, *5A*, 261.

[82] Karim, O. A.; Haymet, A. J.; Banet, M.; Simon, J. D. *J. Phys. Chem.* **1988**, *92*, 3391.

[83] Bader, J. S.; Chandler, D. *Chem. Phys. Lett.* **1989**, *157*, 501.

[84] The difference between this picture and that of outer-sphere electron-transfer reactions—a distinction for which the reagents' nuclear motion is critical—is described in ref 10.

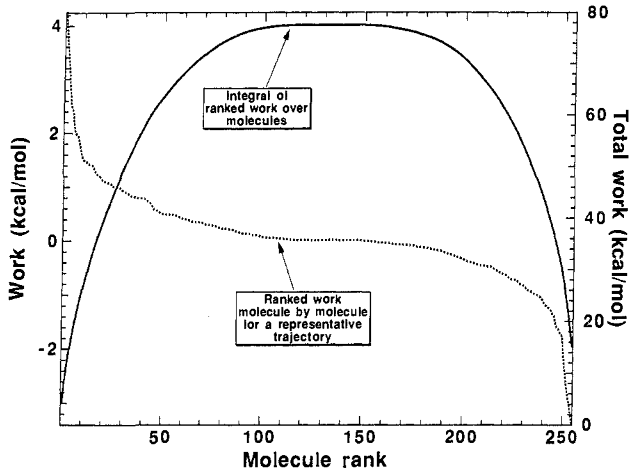

Figure 9. Total work done on the S_N2 reagents for a representative reactive trajectory: work done by individual water molecules over the course of the barrier-climbing process ranked by amount of work done by each solvent molecule (left axis) and integral over molecules of work done in this individual trajectory (right axis).

water molecules. We then rank these molecules by the value of $W_j(t)$, that is, the work done on the reagent atoms up to time t. After ranking the molecules in each trajectory, we average the work done over all the reactive trajectories. We display this quantity as a function of molecule rank in Figure 8 for the work done from −500 to 0, −50, and −200 fs.

The significant feature of Figure 8 is the relatively large number of water molecules doing helping and hindering work. Nearly 20 solvent molecules do more than 1 kcal/mol of helping work over the entire course of the barrier climbing, and, on the other hand, nearly 20 molecules do more than 1 kcal/mol of hindering work. We can also see from Figure 8 that even at times well before the transition state is reached, many solvent molecules have done work on the reagents. In Figure 5, we noted that there was a great deal of helping and hindering work done on each of the reagent atoms. We now see here that each of these types of work is due to the influence of a large number of molecules, rather than just one or two. Once again, we contrast these results to the weak coupling system where very few solvent atoms are involved in the energy transfer and effectively none hinder the reaction process in any significant way.[20]

In Figure 9, we plot the work for a single representative trajectory up to $t = 0$ as a function of molecule rank. In addition, we plot the integral of this quantity over all the solvent molecules. There are two significant features of these curves. First, the ranked work plot for a single trajectory has an essentially identical structure to that of the ranked work averaged over all reactive trajectories. Thus, even for an individual trajectory, there are a large number of water molecules both helping and hindering the progress of the S_N2 reaction.

Second, the integral of the ranked work shows the overall effects of the helping and the hindering water molecules. From Figure 5, we saw that each atom of the S_N2 reagents was having a large amount of both helping and hindering work done on it. Figure 9 presents similar results, but from the perspective of the solvent molecules doing the work. In particular, the helping molecules put almost 80 kcal/mol of energy into the reagents. This amount of helping work is a factor of five greater than that needed to climb the barrier. However, the molecules hindering the reaction are simultaneously withdrawing 65 kcal/mol of energy from the reagents. The conclusion we draw is that there is a violent and rapid competition between many helping and hindering water molecules as the S_N2 reagents climb the barrier. That the reagents actually reach the transition state is the result of a relatively slight predominance of helping work over hindering work.

(Note that Figure 9 is for a single trajectory. This accounts for the change in the total energy of the reagents (15 kcal/mol) being different from that for the statistical average (7 kcal/mol) of Figure 1. Examination of several individual trajectories shows that the change in the total energy of the reagents over the duration of the barrier climb can vary widely. The average change in total energy for the set of reactive trajectories is 7 kcal/mol with a standard deviation of 4.4 kcal/mol. However, the results on the number of molecules involved in the energy flow for an individual trajectory are not dependent on the change in energy of the reagents.)

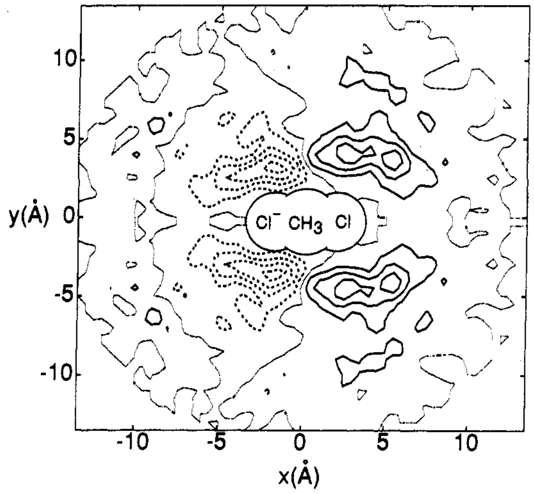

Figure 10. Spatial distribution of work, $W_p(x,y)$, done by the water solvent on the S_N2 reactants as a function of position in Angstroms relative to the S_N2 reagents at $t = 0$. The work done is calculated over the entire barrier-climbing process ($t = -500$ fs to $t = 0$) and segregated into bins based on the position of the oxygen atom of the water solvent molecule. The work distribution is calculated as an average over 100 reactive trajectories and has dimensions of (work/area). $W_p(x,y)$ represents the work done by all molecules in the torus centered at x and with radius y with $x = r \cos \theta$ and $y = r \sin \theta$ where r and θ are as defined in Figure 11. The contours are at equally spaced intervals, but the scale is otherwise arbitrary. Positive contours are solid lines, negative contours are dashed lines, and contours of zero work are dotted lines. The circles represent the approximate average positions of the S_N2 reagent atoms at the transition state. These are labeled as to their nature at the bottom of the barrier to reaction in order to emphasize that the regions of the water solvent doing positive and negative work depend on the identity of the initial chloride ion and initial methyl chloride molecule (see text for details).

Figures 8 and 9 show how *many* molecules do work on the S_N2 system during the barrier-climbing process. An equally interesting problem is to determine *where* the water molecules that do the most work are located relative to the positions of the reactive atoms. Figure 10 presents the beginning of an answer to this problem. In this figure, we display as a contour plot the spatial distribution of work, $W_p(x,y)$ done from $t = -500$ fs to $t = 0$ as a function of water molecule position relative to the reagents. This quantity represents the work done by a particular spatial region of the solvent on all the reactant atoms and is constructed as an average over 100 reactive trajectories. The coordinate system used to define the positions of the water molecules is one that is cylindrically symmetric about an axis perpendicular to the line connecting the positions of the methyl group and the center of mass of the reagents (taken as the origin) at $t = 0$. This defines a coordinate system (r,θ,z) where r is the distance from the center of mass of the reagents to the oxygen atom of a water molecule, θ is the angle between the line of the reagents and the vector connecting the oxygen atom with the center of mass, and z is the distance the oxygen atom is from the plane of the S_N2 reagents. The (r,θ) portion of the coordinate system is sketched in Figure 11. The work done by each water molecule is binned into a specific region of the coordinate system based on the position of the oxygen atom of the water molecule relative to this coordinate system. In Figure 10, the work distribution is displayed as a function of $x = r \cos \theta$ and $y = r \sin \theta$. The value of $W_p(x,y)$ (which has dimensions of work/area) therefore contains the work done by *all* molecules in a torus centered at x and with radius y.[85] The integral of $W_p(x,y)$ over the two coordinates x,y shown

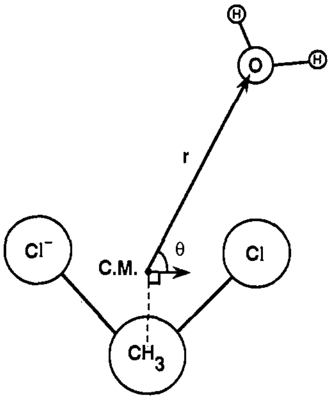

Figure 11. Coordinate system used to calculate work distribution presented in Figure 10. C.M. is the center of mass of the S_N2 reagents at the transition state ($t = 0$). The vector from which θ is measured is perpendicular to the line between the methyl group and C.M. and is in the plane of the S_N2 reagents. Cylindrical symmetry of the system about this vector is assumed. The positions of the circles representing the atoms are schematic, and, as in Figure 10, the atoms are labeled with their identity at the bottom of the potential energy barrier. (Note that at the transition state, the charge distribution is $[Cl^{\delta-}CH_3{}^{\delta+}Cl^{\delta-}]$.)

in Figure 10 therefore gives the total work done on the reactant atoms

$$\int W_p(x,y)\,dx\,dy = E_r(0) - E_r(-500\text{ fs}) \qquad (7)$$

where $E_r(t)$ is the total S_N2 reagent energy at time t. This distribution function represents both water solvent effects due to the strength of the interaction with the S_N2 reagent atoms as well as the cumulative effect of the number of molecules in a given torus.

From Figure 10, we see that the majority of the work done is due to water solvent molecules near the S_N2 reagents, primarily those molecules in the first solvent shell. What is also significant is the clear delineation of helping and hindering work in the conversion $Cl^- + CH_3Cl \rightarrow [Cl^{\delta-}CH_3{}^{\delta+}Cl^{\delta-}]$. The hindering work is entirely localized around the initial chloride ion, while the helping work is localized around the chlorine end of the initial methyl chloride molecule. This result can be readily understood from the change in the S_N2 reagents' charge distribution as they climb the barrier. During this ascent, the initial chloride ion loses almost half of its negative charge. The water solvent molecules that are initially solvating the chloride ion will have their (favorable) interaction with this atom considerably weakened as the reactants approach the transition state. The result is that these water molecules tend to do negative (hindering) work on the reactants. Conversely, the chlorine atom of the initial methyl chloride molecule has its negative charge shift from −0.2 to −0.5 during the barrier climb (cf. Figure 7). The water molecules that are favorably solvating this atom at the bottom of the barrier (albeit weakly) will have a much better interaction when the reactants reach the transition state. These molecules therefore tend to do positive (helping) work on the S_N2 reactants.

This figure further emphasizes the differences between the strong coupling system studied here and the weak coupling system studied earlier.[20] Here, we see that many of the solvent molecules in the inner shell participate in the energy flow to the reagent atoms. In the weak coupling case, only one or two nearby atoms directly participate, with the rest of the solvent behaving largely as spectators.[20] Further analysis of this work distribution should give an even more revealing picture in space and time of how the water solvent transfers energy into the S_N2 reagents.

V. Conclusions

In this and previous papers,[9-12] we have made some progress in understanding how a model S_N2 reaction in aqueous solution takes place where there is a strong interaction between the solvent and the reagents. We summarize here what we have learned of the chronology and characteristics of the climb to the transition state in this reaction.

Over some large time prior to −500 fs (all times are relative to $t = 0$ being the arrival the top of the barrier), the water solvent transfers energy into the methyl chloride molecule causing an average vibrational activation of 10 kcal/mol (a level of $v = 5$). Since we have not examined this prior process here, we need to exploit other considerations to place this activation in perspective for the reaction. Preliminary calculations[86] show that vibrational relaxation of a methyl chloride molecule in water occurs over a time scale of 6–10 ps. This value provides at least a rough estimate for our (nonequilibrium) ensemble of reactive trajectories of how long before reaching the transition state the vibrational excitation began. By using detailed balance arguments and assuming that the vibrational relaxation (activation) rate is the inverse of the vibrational relaxation (activation) time, we estimate the vibrational activation time (the average time for a vibrational excitation to arise in an equilibrium system) to be on the order of 1–10 μs. But this is not the rate-limiting step. As Bergsma et al.[19] have discussed for the Cl + Cl_2 reaction in liquid Ar, the rate constant, k, for a symmetric exchange reaction can be expressed in terms of a vibrational activation rate constant, k_V, and the TST rate constant, k^{TST}, as[8,14,87]

$$k = \frac{k^{TST}}{1 + 2k^{TST}/k_V} \qquad (8)$$

For methyl chloride in water, k_V is on the order of 10^5–10^6 s^{-1},[86] which is far less than k^{TST}.[1] Since $k^{TST} \ll k_V$, the rate constant for the reaction reduces to $k = k^{TST}$ indicating that the barrier passage, and not the vibrational activation, is the rate-limiting step.[19]

Figure 1 shows that from −500 to −350 fs, the methyl chloride has already been vibrationally activated, and little net energy is transferred into the reagents. Note that the reagents are in the solvated ion–dipole complex configuration throughout this time span.

At $t \sim -350$ fs, the kinetic energy of the S_N2 reagents begins to increase steadily and continues to do so until −50 fs. The potential energy of the reagents does not begin to increase appreciably until −100 fs but then continues to increase until −50 fs as well. During this period, a large amount of helping and hindering work is done by the water solvent on the reagent atoms. The work done on the methyl group shows an oscillatory behavior in this time interval with a frequency roughly equal to that of the methyl chloride molecule. While we have not addressed the detailed mechanics of the energy transfer into the reagents during this time span, this oscillatory behavior is indicative of an effective coupling of the vibrational motions of the ion–dipole complex with similar frequency motions in the water solvent.

The time span from $t = -50$ fs to $t = 0$ is characterized by an extremely rapid climb of the S_N2 reagents to the top of the barrier. The kinetic energy of the reagents is converted almost completely to potential energy. (Since at $t = 0$ there is a canonical ensemble in all degrees of freedom except the reaction coordinate, there is a thermal distribution of kinetic energy in the reagents at the top of the barrier.) The system then undergoes the dynamics near the top of the barrier described more completely in previous work.[9,10,12]

From the point of view of the water solvent, the chronology is somewhat different. From −500 to −20 fs, we observe a steady decrease in the total energy of the water. Further analysis shows that this decrease is primarily in the intermolecular potential energy of the water, while a smaller decrease in water kinetic energy is also observed. This partitioning can be understood in

---

[85] We add up all the work done by all the water molecules in a given torus; there is no prior division made into helping and hindering work. Therefore, Figure 10 displays net work. In addition, a cylindrical symmetry is assumed in generating the work distribution that is only approximately present in the actual system due to the noncollinearity of the reagents. However, because the reagents do not deviate by more than ~20° from collinearity over the course of the barrier climbing process, this assumption is qualitatively reasonable.

[86] Whitnell, R. M.; Wilson, K. R.; Hynes, J. T. *J. Phys. Chem.*, in press.

[87] Northrup, S. H.; Hynes, J. T. *J. Chem. Phys.* **1980**; *73*, 2700.

terms of a thermodynamic model based on heat capacity. Concomitantly, the potential energy of solvent–reagent interaction increases over this time span. We interpret these changes as a reorganization[6,7,9–11,88] of the water solvent molecules so that they can appropriately solvate the symmetric charge distribution of the S_N2 reagents at the transition state ($Cl^{\delta-}CH_3^{\delta+}Cl^{\delta-}$) rather than the more localized negative charge of the ion–dipole complex (Cl^-CH_3Cl). However, this structural change in the solvent has almost entirely occurred *before* the charge distribution within the reactants has undergone any significant change from that of the ion–dipole complex.[84] The water solvent reorganization observed here certainly has some relationship to the more general notion of a "solvent coordinate"[8,14–17] for heavy-particle charge-transfer reactions. A number of studies of the dynamics of this S_N2 reaction have invoked a solvent coordinate in order to understand the transmission coefficient and the dynamics near the transition state[10–12,30,40,41] as well as some features of the barrier-climbing dynamics.[6,7]

In the last 20 fs of the barrier-climbing process, the solvent can be viewed as essentially frozen. The change in the reactants as they climb the barrier happens so swiftly that the solvent cannot adiabatically respond. The results presented here are in complete accord with the frozen solvent nonadiabatic solvation model[10,15–17,40,41] used previously to understand the transition-state dynamics and barrier-recrossing phenomena observed for this S_N2 system first calculated in molecular dynamics simulations[9,10,12] and later computed via integral equation methods.[4] In this 20 fs time span, we observe some energy loss out of the reactants into the solvent–reagent potential energy, and we interpret this loss as a deceleration by the frozen solvent of the chloride ion as its charge is reduced during the climb of the barrier.

In addition to a detailed knowledge of the energetics of this reaction, we have also gained an understanding of some of the more general energy-transfer aspects of the aqueous solvent contribution to this reaction process (in addition to the reorganizational features described above). Many water solvent molecules are involved in the energy transfer to the S_N2 reagents as measured by the work done on the reagent atoms. However, not all of the participating solvent molecules help the reaction occur. We observe that a significant number hinder the reaction. Finally, in examining the work done over the entire barrier-climbing process ($Cl^- + CH_3Cl \rightarrow [Cl^{\delta-}CH_3^{\delta+}Cl^{\delta-}]$), we see a division of net helping and hindering work into different regions of the solvent. Hindering work is concentrated around the chloride ion; helping work is concentrated around the chlorine of the methyl chloride molecule. The majority of this work is done by water molecules in the first solvent shell, and the spatial distribution of the molecules doing the helping and hindering work has been explained in terms of the movement of charge during the barrier ascent from the initial chloride ion to the chlorine atom of the methyl chloride molecule. As this charge shifts, water solvent molecules that are initially solvating the chloride ion will have that favorable interaction weakened as the magnitude of the charge on that atom lessens. This decreasing interaction results in these solvent molecules doing hindering work on the reagents. On the other hand, water molecules that are weakly solvating the chlorine atom of the initial methyl chloride molecule will have their interaction with this chlorine strengthened during the climb of the barrier and will therefore tend to do helping work on the S_N2 reagents.

We again note that this system is a *model* of an S_N2 reaction in water. However, since many qualitative features of the reactant and solvent models used here appear in the actual S_N2 reaction in water, we expect that the behavior of the energy flow (time scales, number of water molecules involved, etc.) observed in these calculations will carry over to more accurate models of this reaction as well as to the experimental aqueous reaction. We do not expect that the consideration of more detailed models of the reaction system, such as those containing all 18 degrees of freedom of the six atom system,[46,47] or of the solvent will change our qualitative conclusions. (The detailed quantitative results will, of course, be different.)

We wish again to point out the large differences between this (strong coupling) model S_N2 system in water and the (weak coupling) model $Cl + Cl_2$ system in liquid Ar[19] whose energy flow patterns were studied in detail by Benjamin et al.[20] Even though the time scale over which the reactant barrier-climbing process occurs is similar for the two reactions, the mechanism of energy transfer from solvent to reactants is very different. In the weak coupling case, energy transfer is dominated by transfer of kinetic energy through impulsive collisions of solvent and reagent atoms. Very few solvent atoms are directly involved in this energy transfer, and cases where a solvent atom significantly hinders the reaction are very rare.

In the strong coupling system, the energy transfer is dominated by potential energy interactions involving a large number of water solvent molecules. In addition, we see a competition between those solvent molecules that help the S_N2 reaction occur and those that hinder the reaction. Through comparison of the time scales of the changes in the reagent–solvent and solvent intermolecular potential energy with the time scales for reagent potential energy change and reagent charge redistribution, we infer that the water solvent undergoes a reorganization prior to the fast climb of the S_N2 reagent potential energy barrier and the concomitant change in the charge distribution among the reagent atoms. The prior reorganization observed in this strong coupling system is needed for a successful climb of the barrier, in contrast to the weak coupling system. Finally, as has been known from previous work,[9,10,12] the transition-state dynamics and significant barrier recrossings in the strong coupling S_N2 system can be treated by using a frozen solvent nonadiabatic solvation model.[9,10,12,15–17] The water solvent has been demonstrated to have very important effects in the S_N2 system even in the very short time span during which the transition-state dynamics take place. In the weak coupling system,[19] where essentially no barrier recrossings occur, the effect of the solvent on the transition-state dynamics is almost nonexistent.

It is also useful to note several similarities between the S_N2 and $Cl + Cl_2$ model systems. Both systems exhibit vibrational excitation in the diatomic molecule well before energy flows into other reactant modes.[9,19] In addition, the energy beyond vibrational activation needed to surmount the barrier flows into the reagents over an ~200 fs time scale with the final rapid climb of the barrier occurring in the last ~50 fs. Some of this behavior may be due to a strong influence of the similar gas-phase potentials for the two sets of reagents.

In this work, we have described the energetics of a model S_N2 barrier-climbing process in detail and used this description to understand many aspects of the dynamics. Future efforts will be aimed toward a further understanding of several structural (spatial and temporal) aspects of these dynamics in order to comprehend further the reaction mechanism. These include the overall structure of the water solvent and its evolution as the solvation of the reagents changes as well as the spatial distribution of those water molecules that contribute to the energy flow during the different time spans we have discussed. These investigations should give a more complete picture of how both the solvent and the reagents (and the interactions between the two) determine the mechanism of the reaction process.

Acknowledgment is made to the donors of the Petroleum Research Fund, administered by the American Chemical Society, for partial support of this work (J.T.H.). We also thank the National Science Foundation for support of this research through a grant to J.T.H. (CHE88-07852) and through a Graduate Fellowship to B.J.G. We thank Ilan Benjamin for useful discussions.

Appendix

The preparation of the independent seeds and the initial conditions for the system containing 64 water molecules is described in detail by Gertner et al.[12] We first review that method here.

---

(88) Hynes, J. T. *Discuss. Faraday Soc.* **1988**, *85*, 347.
(89) Nosé, S. *Mol. Phys.* **1984**, *52*, 255.

We wish to start the trajectories with the reagents at the transition-state value of the reaction coordinate and to sample all other degrees of freedom from a canonical ensemble. For the 64 water molecule case, this was done by placing the $Cl^- + CH_3Cl$ system in the center of the box and surrounding it with the water molecules added one by one. The positions and orientations of the water molecules were chosen randomly, rejecting any attempted placement that significantly overlapped with any of the molecules already placed in the box. The size of the box was chosen to obtain the desired density (in this case 1.0 g cm^{-3}). The asymmetric stretch of the $Cl^- + CH_3Cl$ system was then constrained to be zero (corresponding to the transition state of the system), and the potential energy of the entire system was minimized with respect to all other degrees of freedom. The system was then equilibrated to the appropriate temperature (298 K) over a period of 5 ps by using an algorithm which randomizes the velocities (sampling from the Maxwell–Boltzmann distribution) every 0.25 ps. During this equilibration, the value of the reaction coordinate (eq 5) of the reagents and the velocity of this degree of freedom were constrained to be zero. Ten independently created and equilibrated "seeds" were thereby produced by Gertner et al.[12] and were used to generate a total of 400 sets of initial configurations through a continuation of the dynamics and equilibration process.

We use 10 of these 64 water molecule initial condition files (one from each of the original independently created seeds) to generate the 256 water molecule initial condition files. In order to keep the same density of 1.0 g cm^{-3}, the unit cell for the 256 water molecule system must be a factor of $4^{1/3}$ larger than that for the 64 molecule system. For each of the 64 water initial condition files, we calculate the 14 closest periodic images (one for each face of the truncated octahedron) and retain only those molecules that lie within the appropriate unit cell for the 256 water system, randomly removing excess water molecules if the total is larger than 256. (This new system includes all the molecules in the original system.) By virtue of how it is constructed, this larger system has no unfavorable molecule–molecule interactions within its boundaries as it would if molecules were placed in it randomly. However, the molecules on the surface of the original (64 water) unit cell may interact unfavorably with periodic images of other solvent molecules. In order to correct this, we first increase the size of the unit cell by ~1 Å, in effect placing some vacuum around the system. Five hundred fs of constant temperature dynamics using the Nosê algorithm[89] is then run during which time the system expands into the larger volume. In the process, the unfavorable interactions with the periodic images are eliminated. Since this system is now at the wrong density, the linear dimensions of the unit cell are compressed by 2%, all solvent atom positions are also scaled by that factor, and constant temperature dynamics are run on the compressed system for 500 fs to equilibrate the system at the new volume. This compression–equilibration process is repeated until the original desired density is regained. This equilibration should also be sufficient to remove any traces of the symmetry remaining in the original system bootstrapped from the mosaic of smaller systems.

Theoretical Studies on the Ring-Opening Reactions of Bicycloalkyl Radicals: Homolytic β-Scission in Bicyclo[1.1.0]but-2-yl Radical

Santiago Olivella*,[†] **and Albert Solê**

Contribution from the Departments de Quîmica Orgânica and Quîmica Fîsica, Universitat de Barcelona, Martî i Franquès 1, 08028-Barcelona, Catalunya, Spain. *Received April 30, 1990*

Abstract: Ab initio UHF and CASSCF calculations have been performed on the two modes of ring opening in bicyclo[1.1.0]but-2-yl radical (**8**), involving homolytic β scission of a C–C bond. Although the fusion bond cleavage in **8** to give cyclobutenyl radical (**9**) is formally an orbital-symmetry-forbidden electrocyclic process, the activation energy is calculated to be only ≈3 kcal/mol. This ring opening is predicted to take place via a highly nonsymmetric transition structure, which allows the mixing of the SOMO (a′ symmetry) and LUMO (a″ symmetry) of **8**, and the coupling between the crossing states (2A′ and 2A″), resulting in an adiabatic reaction on the ground-state potential surface. The alternative β-scission mode in **8**, involving cleavage of an outer cyclopropane bond to afford cyclopropenylmethyl radical (**10**), is predicted to have an activation energy of ≈26 kcal/mol. Although the partial breaking of such a peripheral bond in the transition state involves a great relief of the strain energy of the cyclopropane moiety in **8**, this is nearly compensated by the increase of strain energy that takes place simultaneously in the cyclopropyl ring of **8** because the partial making of an inner double bond.

I. Introduction

Radical species containing small strained bicycloalkyl structures are interesting because the rigid framework of carbon atoms can lead to unusual and even unprecedented chemical behavior. The presence of a large amount of strain energy makes the ring opening by cleavage of a β, γ C–C bond with respect to the radical center (i.e., β scission) a common process. In the case of bicyclo[*n*.1.0]alk-2-yl radicals (**1**), there are two types of β,γ C–C bonds and, therefore, two different modes of β scission can be envisaged (Scheme I). Thus, β scission of the fusion bond (mode 1) gives cycloalkenyl radicals (**2**), while β scission of the outer cyclopropane bonds (mode 2) would yield cycloalkenylmethyl radicals (**3**).

It has been pointed out that ring opening by β scission readily occurs in cycloalkyl radicals if the semioccupied molecular orbital (SOMO) can assume an eclipsed conformation with respect to the β,γ bond; namely, there is strong overlap between the SOMO and the orbitals of the bond about to break.[1] This stereoelectronic

Scheme I

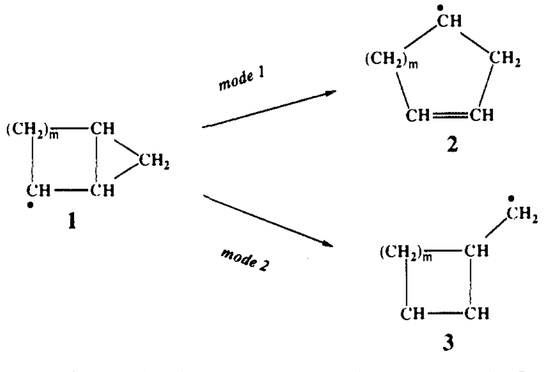

[†] CSIC Research Professor.

0002-7863/91/1513-87$02.50/0